

Gamma-ray bursts as cosmological probes: Λ CDM vs. conformal gravity

Antonaldo Diaferio,^{a,b,c} Luisa Ostorero,^{a,b,d,c} and Vincenzo Cardone^e

^aDipartimento di Fisica Generale “Amedeo Avogadro”, Università degli Studi di Torino, Via P. Giuria 1, I-10125, Torino, Italy

^bIstituto Nazionale di Fisica Nucleare (INFN), Sezione di Torino, Via P. Giuria 1, I-10125, Torino, Italy

^cHarvard-Smithsonian Center for Astrophysics, 60 Garden Street, Cambridge, MA 02138, USA

^dDepartment of Physics and Astronomy, University of Pennsylvania, 209 South 33rd Street, Philadelphia, PA 12104, USA

^eINAF - Osservatorio Astronomico di Roma, via Frascati 33, 00040, Monte Porzio Catone, Roma

E-mail: diaferio@ph.unito.it, ostorero@ph.unito.it, winyenodrac@gmail.com

Abstract. Λ CDM, for the currently preferred cosmological density Ω_0 and cosmological constant Ω_Λ , predicts that the Universe expansion decelerates from early times to redshift $z \approx 0.9$ and accelerates at later times. On the contrary, the cosmological model based on conformal gravity predicts that the cosmic expansion has always been accelerating. To distinguish between these two very different cosmologies, we resort to gamma-ray bursts (GRBs), which have been suggested to probe the Universe expansion history at $z > 1$, where identified type Ia supernovae (SNe) are rare. We use the full Bayesian approach to infer the cosmological parameters and the additional parameters required to describe the GRB data available in the literature. For the first time, we use GRBs as cosmological probes without any prior information from other data. In addition, when we combine the GRB samples with SNe, our approach neatly avoids all the inconsistencies of most numerous previous methods that are plagued by the so-called circularity problem. In fact, when analyzed properly, current data are consistent with distance moduli of GRBs and SNe that can respectively be, in a variant of conformal gravity, ~ 15 and ~ 3 magnitudes fainter than in Λ CDM. Our results indicate that the currently available SN and GRB samples are accommodated equally well by both Λ CDM and conformal gravity and do not exclude a continuous accelerated expansion. We conclude that GRBs are currently far from being effective cosmological probes, as they are unable to distinguish between these two very different expansion histories.

Keywords: modified gravity – gamma rays burst experiments – dark energy experiments – supernova type Ia - standard candles

Contents

1	Introduction	1
2	Cosmology in Conformal Gravity	3
2.1	Conformal Gravity (CG)	3
2.2	Kinematic Conformal Cosmology (KCG)	8
3	Bayesian analysis	11
3.1	GRB sample	11
3.2	SN sample	14
3.3	GRBs combined with SNe	17
4	Discussion	19
5	Conclusion	22
A	Bayesian analysis	24
A.1	Bayesian parameter estimation	24
A.2	Bayesian model selection	25
A.3	Numerical details	26

1 Introduction

The evidence of the accelerated expansion of the Universe coming from extensive surveys of high-redshift type Ia supernovae (SNe) in the late 1990s [1, 2] can be accurately described by a non-zero cosmological constant Λ in Friedmann equations. For reasons that might not be fully convincing [3–5], this simple solution does not satisfy a large fraction of the scientific community. Thus, more sophisticated models have been proposed: from arbitrary modifications of the Einstein-Hilbert action in $f(R)$ models to brane-world cosmologies with extra spatial dimensions in addition to the standard four dimensional space-time, to mention a few [see, e.g., 6–8, for reviews]. Despite their wildly different starting point, all these models were conceived to describe the SN data and reproduce the expansion history of a standard Λ Cold Dark Matter (Λ CDM) universe. Therefore, these models are expected to have a decelerated period followed by the present accelerated phase. In the Λ CDM model, the transition occurs at redshift $1 + z = (2\Omega_\Lambda/\Omega_0)^{1/3}$, where Ω_0 is the present average mass density and Ω_Λ the energy density associated to the cosmological constant. According to recent measures of these parameters [e.g., 9], this transition redshift is $z \approx 0.9$.

Before high- z SN surveys were performed, the number of cosmological models alternative to the standard Friedman model was very limited. Notably, the steady-state cosmology required an accelerated expansion more than forty years earlier [10]. Before the detection of the accelerated expansion, Mannheim [11] also proposed conformal gravity as a cosmological model, without a cosmological constant, that was alternative to the standard de Sitter solution. After the high- z SN observations, Mannheim [12, 13] showed how conformal gravity can easily describe these data. Therefore, unlike recent alternative cosmologies, the steady-state model and conformal gravity have the remarkable property that the accelerated expansion is a natural feature of the model and not a requirement for building the theory.

Conformal gravity requires that the expansion of the Universe has always been accelerating and a deceleration phase never occurred. Thanks to this prediction, substantially different from Λ CDM, conformal gravity is an ideal candidate to test whether the claimed transition between the decelerated and accelerated expansion expected in Λ CDM is robust. A potentially clean and powerful test to verify the existence of a decelerating phase in the early Universe is to extend the Hubble diagram of SNe to very high redshifts. Unfortunately, SNe are rarely observed at z larger than 1, and gamma-ray bursts (GRBs) were instead proposed as possible candidates to probe this high-redshift regime. The first sufficiently accurate estimates of the celestial coordinates of GRBs provided by BeppoSAX [14] enabled the measure of the host galaxy redshift and proved the extragalactic origin of GRBs. This breakthrough immediately prompted the discussion of how we can use GRBs to constrain the cosmological model: for example, Cohen and Piran [15] discussed how GRBs with known redshift could be used to estimate Ω_0 . Atteia [16] also suggested to use GRBs as standard candles based on the intrinsic dispersion of various measures of the GRB brightness.

A crucial step forward was the discovery that the luminosity of GRBs appears to be correlated with some of their temporal and spectral properties that can be directly observed on Earth [e.g., 17–19]. These correlations are not yet fully understood from first physical principles. However, their existence has naturally suggested the use of GRBs as distance indicators [20, 21]. GRBs have been observed out to redshift $z = 8.2$ [22, 23] and are expected to be observed to even larger redshifts in the future [24, 25]. They could thus be a powerful cosmological probe of the early history of the Universe expansion (see, e.g., [26] for an early review).

The obvious procedure to use GRBs as distance indicators has two steps: (1) calibrate the correlations, and (2) use the calibrated correlations to estimate the GRB luminosity distances of a given sample. We can thus build the GRB Hubble diagram and eventually constrain the cosmological model. This procedure has an immediate drawback. Unlike SNe, there are no observed nearby GRBs and the calibration of a given correlation with a GRB sample requires the assumption of a cosmological model to estimate the GRB luminosities from their fluxes and redshifts. In principle, within the framework of a given cosmological model, these correlations might be used to infer the luminosities, and hence the luminosity distances, of other GRBs for which the remaining variable of the correlation is known. However, using these luminosity distances to constrain a cosmological model different from the model used to calibrate the correlations clearly poses a problem of consistency.

A more appropriate approach is to extract, at the same time, the correlation coefficients and the cosmological parameters of the model from the observed quantities. To accomplish this task, it is sufficient to lay out the problem within a full Bayesian context and use Markov Chain Monte Carlo (MCMC) simulations to compute, simultaneously, the full probability density functions (PDFs) of all the parameters of interest. This approach does not require any prior information on the cosmological model and yields results that are not plagued by any of the various limitations found in the literature [e.g., 27–34]. In addition, we are able to test cosmological models both with GRBs alone, without any priors from other probes, and by combining GRBs with other observables.

Here we apply the Bayesian analysis to the GRB sample, the SN sample, and the GRB and SN samples combined (sect. 3), after reviewing the basic ingredients of the conformal gravity cosmological model in sect. 2. We discuss our results in sect. 4 and conclude in sect. 5.

2 Cosmology in Conformal Gravity

We investigate two variants of conformal gravity: the model proposed by Mannheim [11], that we will indicate with CG, and the kinematic conformal gravity (KCG) proposed by Varieschi [35].

CG, which is a simplified version of the original Weyl's theory [36–38], describes the rotation curves of disk galaxies without resorting to dark matter [39–41]. In addition, CG is appealing because it appears to be a renormalizable theory of gravitation [42, 43] and it is therefore suggestive of a possible route towards the unification of the fundamental forces; moreover, unlike other fourth-order derivative theories, CG does not suffer from the presence of ghosts [44]. However, as we mentioned above, in CG the universe has been accelerating at all times and never went through a deceleration phase. This very fact implies that the primordial nucleosynthesis lasts for a more extended time interval than in the standard model and the expected abundance of primordial deuterium is orders of magnitudes smaller than observed [45, 46]. This shortcoming of CG can be bypassed if astrophysical processes, rather than cosmological nucleosynthesis, supply the abundance of deuterium currently observed: the question is open, because the investigation of the efficiency of all the possible mechanisms producing deuterium is still incomplete [47].

KCG derives from the kinematical application of the conformal symmetry to the Universe and implies a physical interpretation of the cosmological observables radically different from the standard model, as we will see below. In principle, similarly to CG, KCG does not require the presence of dark matter, dark energy, and an inflationary phase. In addition, KCG naturally explains the anomalous Pioneer acceleration [48].

We describe the basic properties of the CG and KCG cosmological models below.

2.1 Conformal Gravity (CG)

In CG¹ the field action is [11]

$$I_W = -\alpha \int d^4x \sqrt{-g} C_{\mu\nu\kappa\lambda} C^{\mu\nu\kappa\lambda} \quad (2.1)$$

where $C_{\mu\nu\kappa\lambda}$ is the Weyl tensor, α is a coupling constant, and g is the determinant of the metric tensor $g_{\mu\nu}$.

The field equations are

$$4\alpha W^{\mu\nu} = T^{\mu\nu} \quad (2.2)$$

with $T^{\mu\nu}$ the energy-momentum tensor and

$$\begin{aligned} W^{\mu\nu} = & -\frac{1}{6}g^{\mu\nu}R_{;\lambda}^{\lambda} + \frac{2}{3}R^{;\mu;\nu} + R_{;\lambda}^{\mu\nu;\lambda} + \\ & -R_{;\lambda}^{\nu\lambda;\mu} - R_{;\lambda}^{\mu\lambda;\nu} + \frac{2}{3}RR^{\mu\nu} + \\ & -2R^{\mu\lambda}R_{\lambda}^{\nu} + \frac{1}{2}g^{\mu\nu}R_{\lambda\kappa}R^{\lambda\kappa} - \frac{1}{6}g^{\mu\nu}R^2 \end{aligned} \quad (2.3)$$

where $R^{\mu\nu}$ and R are the Ricci tensor and scalar, respectively.

The matter action can take the form [49, 50]

$$I_M = - \int d^4x \sqrt{-g} \left\{ \frac{1}{2}S^{;\mu}S_{;\mu} - \frac{1}{12}S^2R + \right.$$

¹We use natural units with $\hbar = c = 1$.

$$+ \lambda S^4 + i\bar{\psi}\gamma^\mu[\partial_\mu + \Gamma_\mu]\psi - hS\bar{\psi}\psi\} \quad (2.4)$$

where $S(x)$ is a scalar field introduced to spontaneously break the conformal symmetry, $\psi(x)$ is a fermion field representing all matter, $\Gamma_\mu(x)$ is the fermion spin connection, $\gamma^\mu(x)$ are the general relativistic Dirac matrices, and h and λ are dimensionless coupling constants. The above action can be extended to include more than one scalar field [12]. The first three terms in the action are generated with an effective Ginzburg-Landau theory where $S(x)$ is a phase transition condensate order parameter. Specifically, the term λS^4 represents the negative minimum of the Ginzburg-Landau potential, namely the vacuum energy density [12]. It follows that we must have $\lambda < 0$.²

With this action and its matter and scalar field equations, the generic energy-momentum tensor is

$$\begin{aligned} T^{\mu\nu} = & i\bar{\psi}\gamma^\mu[\partial^\nu + \Gamma^\nu]\psi + \frac{2}{3}S^{;\mu}S^{;\nu} - \frac{1}{6}g^{\mu\nu}S^{;\kappa}S_{;\kappa} \\ & - \frac{1}{3}SS^{;\mu;\nu} + \frac{1}{3}g^{\mu\nu}SS^{;\kappa}_{;\kappa} \\ & - \frac{1}{6}S^2\left(R^{\mu\nu} - \frac{1}{2}g^{\mu\nu}R\right) - g^{\mu\nu}\lambda S^4. \end{aligned} \quad (2.5)$$

Using local conformal invariance, we can set $S = S_0 = \text{const}$ and the energy-momentum tensor becomes

$$T^{\mu\nu} = T_{\text{kin}}^{\mu\nu} - \frac{1}{6}S_0^2\left(R^{\mu\nu} - \frac{1}{2}g^{\mu\nu}R\right) - g^{\mu\nu}\lambda S_0^4 \quad (2.6)$$

where $T_{\text{kin}}^{\mu\nu} = i\bar{\psi}\gamma^\mu[\partial^\nu + \Gamma^\nu]\psi$.

Moreover, in the Friedmann-Robertson-Walker (FRW) metric

$$ds^2 = -dt^2 + a^2(t)\left[\frac{dr^2}{1-kr^2} + r^2(d\theta^2 + \sin^2\theta d\phi^2)\right], \quad (2.7)$$

$W^{\mu\nu} = 0$ and equation (2.2) implies $T^{\mu\nu} = 0$, namely

$$\frac{S_0^2}{6}\left(R^{\mu\nu} - \frac{1}{2}g^{\mu\nu}R\right) = T_{\text{kin}}^{\mu\nu} - g^{\mu\nu}\lambda S_0^4. \quad (2.8)$$

For an energy-momentum tensor of a perfect fluid, $T_{\text{kin}}^{\mu\nu} = (\rho + p)u^\mu u^\nu + pg^{\mu\nu}$, equation (2.8) is similar to Einstein cosmic equations recast in the form³

$$-\frac{1}{8\pi G}\left(R^{\mu\nu} - \frac{1}{2}g^{\mu\nu}R\right) = T^{\mu\nu} - g^{\mu\nu}\Lambda' \quad (2.9)$$

where the usual cosmological constant $\Lambda = 8\pi G\Lambda'$. It follows that, in conformal cosmology, G is replaced by the negative quantity $-3/(4\pi S_0^2)$ and the usual cosmological constant $\Lambda = 8\pi G\Lambda'$ by the quantity $-6\lambda S_0^2$, where $\Lambda' = \lambda S_0^4$.

Equation (2.8) and a perfect fluid energy-momentum tensor yield the differential equation for the scale factor a

$$\dot{a}^2 + k = -\frac{2\rho a^2}{S_0^2} - 2\lambda S_0^2 a^2 \quad (2.10)$$

²We note that this sign is opposite to the requirement $\lambda > 0$ of Mannheim [49] and Elizondo and Yepes [46].

³We use the Weinberg [51] sign convention.

which is identical to the standard Friedmann equation ($\dot{a}^2 + k = 8\pi G\rho a^2/3 + \Lambda a^2/3$) with the proper substitutions $G = -3/(4\pi S_0^2)$ and $\Lambda = -6\lambda S_0^2$ mentioned above. These substitutions make the fundamental difference with the standard Friedmann models, because in CG both G and Λ' are negative rather than positive. Moreover, G and Λ' depends on the same parameter S_0^2 , and they depend on it in the opposite way: the lower is the gravitational cosmic repulsion (because G is negative), the larger is the absolute value of the vacuum energy density Λ' . Finally, CG is able to describe the flat rotation curves of spiral galaxies with the aid of a universal constant γ_0 , which is related to the geometric parameter k of the FRW metric by the relation $\gamma_0^2 = -4k$ [40]. Therefore, we need to have $k < 0$.

In equation (2.10), we can separate the matter/energy density into a relativistic and a non-relativistic component: $\rho = \rho_{\text{nr}} + \rho_{\text{r}} = \rho_{\text{nr}0}(a_0/a)^3 + \rho_{\text{r}0}(a_0/a)^4$; the dependence on a derives from the conservation of the energy-momentum tensor of a perfect fluid with an equation of state $p = w\rho$, with $w = 0$ and $w = 1/3$ for the non-relativistic and relativistic components, respectively; in the FRW metric, this equation of state implies $\rho a^{3(w+1)} = \text{const.}$

We define

$$\begin{aligned}\Theta_{\text{m}} &\equiv \frac{2\rho}{H^2 S_0^2} = \Theta_{\text{nr}} + \Theta_{\text{r}} \equiv \frac{2\rho_{\text{nr}}}{H^2 S_0^2} + \frac{2\rho_{\text{r}}}{H^2 S_0^2}, \\ \Theta_{\Lambda} &\equiv -\frac{2\lambda S_0^2}{H^2}, \\ \Theta_k &\equiv -\frac{k}{H^2 a^2},\end{aligned}\tag{2.11}$$

where $H = \dot{a}/a$. All these parameters are positive because $\lambda < 0$ and $k < 0$. Equation (2.10) yields

$$\Theta_{\Lambda} + \Theta_k - \Theta_{\text{nr}} - \Theta_{\text{r}} = 1.\tag{2.12}$$

Unlike the standard cosmology, the expansion of the scale factor in the conformal universe accelerates at all times. In fact, by taking the derivative of equation (2.10), we get

$$\ddot{a} = H^2 a \left(\frac{\Theta_{\text{nr}}}{2} + \Theta_{\text{r}} + \Theta_{\Lambda} \right)\tag{2.13}$$

which is always positive, whereas the deceleration parameter

$$q \equiv -\frac{\ddot{a}a}{\dot{a}^2} = -\frac{\Theta_{\text{nr}}}{2} - \Theta_{\text{r}} - \Theta_{\Lambda}\tag{2.14}$$

is always negative.

By labelling the Θ parameters at the present time t_0 with the “0” subscript, we can rewrite equation (2.10) as

$$\dot{a}^2 a^2 = H_0^2 (\Theta_{\Lambda 0} a^4 + \Theta_{k 0} a^2 - \Theta_{\text{nr} 0} a - \Theta_{\text{r} 0}).\tag{2.15}$$

Again, equation (2.15) is analogous to the standard Friedmann equation

$$\dot{a}^2 a^2 = H_0^2 (\Omega_{\Lambda 0} a^4 + \Omega_{k 0} a^2 + \Omega_{\text{nr} 0} a + \Omega_{\text{r} 0})\tag{2.16}$$

with the standard $\Omega_{\text{nr} 0, \text{r} 0} = 8\pi G\rho_{\text{nr} 0, \text{r} 0}/3H_0^2$, $\Omega_{\Lambda 0} = \Lambda/3H_0^2$, and $\Omega_{k 0} = \Omega_{\text{nr} 0} + \Omega_{\text{r} 0} + \Omega_{\Lambda 0} - 1$.

The main difference between the standard equation (2.16) and its conformal counterpart (equation 2.15) is the negative sign in front of the matter parameters $\Theta_{\text{nr} 0}$ and $\Theta_{\text{r} 0}$. The left-hand side is always positive; therefore, to have real solutions for $a(t)$, the sum of the first

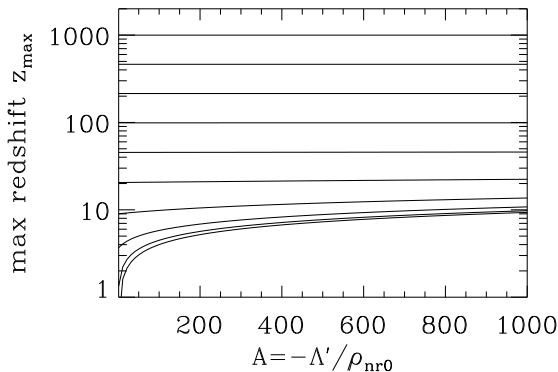


Figure 1. Dependence of the maximum observable redshift z_{\max} on the parameters A and B in equation (2.17). From bottom to top, the curves are for increasing $B = -k/(\rho_{\text{nr}0}S_0^2a_0^2)$ in the range 1 – 1000, logarithmically spaced.

two terms on the right-hand side of equation (2.15) must always be larger than the sum of the latter two. On the contrary, in equation (2.16), for sufficiently small a , the matter terms dominate and we have the usual solutions $a \propto t^{1/2}$, when $\Omega_{\text{nr}0}a$ is negligible in the radiation dominated epoch, and $a \propto t^{2/3}$ in the matter dominated epoch, at somewhat larger a 's.

Therefore, in CG, a never reaches the singularity $a = 0$, but rather a lower limit $a_{\min} > 0$ that is the root of the equation $\Theta_{\Lambda 0}a^4 + \Theta_{k0}a^2 - \Theta_{\text{nr}0}a - \Theta_{\text{r}0} = 0$. In the real Universe we can observe objects at very high redshift, $z > 8$ [e.g., 52]. Thus, we must have $a_{\min} = 1/(1 + z_{\max}) < 0.1$, or possibly smaller. To obtain sufficiently small roots a_{\min} , we can set larger and larger $\Theta_{\Lambda 0}$ and smaller and smaller $\Theta_{\text{nr}0}$ and $\Theta_{\text{r}0}$.

To understand how a_{\min} depends on the Θ conformal cosmological parameters, we can consider that $\rho_{\text{r}0}$, the density of the Cosmic Microwave Background, is $\rho_{\text{r}0} \sim 10^{-34} \text{ g cm}^{-3}$ [9]. To estimate $\rho_{\text{nr}0}$ we consider only the contribution of the luminous component of the galaxies and assume a mass-to-light ratio $M/L \sim 1$, because CG, in principle, does not require the existence of any dark matter [39]. We find $\rho_{\text{nr}0} \sim 10^{-32} \text{ g cm}^{-3}$. Therefore $\Theta_{\text{r}0}/\Theta_{\text{nr}0} = \rho_{\text{r}0}/\rho_{\text{nr}0} \sim 10^{-2}$ and we can neglect the last term in equation (2.15), which becomes

$$\dot{a}^2 a = H_0^2 \Theta_{\text{nr}0} (Aa^3 + Ba - 1) \quad (2.17)$$

where $A = \Theta_{\Lambda 0}/\Theta_{\text{nr}0} = -\Lambda'/\rho_{\text{nr}0}$, and $B = \Theta_{k0}/\Theta_{\text{nr}0} = -k/(\rho_{\text{nr}0}S_0^2a_0^2)$. With this approximation, $a_{\min} = [(1+Q)^{1/3} + (1-Q)^{1/3}]/(2A)^{1/3}$, where $Q = \sqrt{1 + 4B^3/27A}$. When $B \rightarrow \infty$, $a_{\min} = 1/B$, whereas when $B \rightarrow 0$, $a_{\min} = 1/A^{1/3}$. Figure 1 shows the dependence of z_{\max} on A and B . Clearly, sufficiently large A and B , with no specific fine tuning, can easily accommodate the observations of high- z objects.

For a sufficiently large scale factor a , we can also drop the last term in equation (2.17) and replace equation (2.15) with

$$\dot{a}^2 = H_0^2 (\Theta_{\Lambda 0}a^2 + \Theta_{k0}) . \quad (2.18)$$

The integration of this equation trivially is

$$a(t) = \sqrt{\frac{\Theta_{k0}}{\Theta_{\Lambda 0}}} \sinh y \quad (2.19)$$

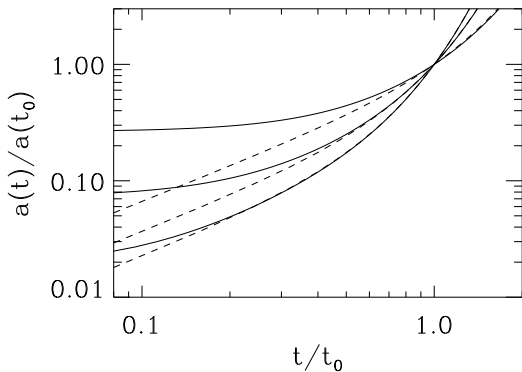


Figure 2. Evolution of the scale factor $a(t)$ for different z_{\max} : from top to bottom the solid lines are for $z_{\max} = 2.8, 13, 53$. The dashed lines show the corresponding $a(t)$ when the matter terms $\Theta_{\text{nr}0}$ and $\Theta_{\text{r}0}$ are neglected. These approximated solutions have the same $H_0 t_0$ of the exact solutions.

with $y = \sqrt{\Theta_{\Lambda 0}} H_0 t$. Clearly, this solution is invalid when $a \rightarrow a_{\min}$. By imposing $a(t_0) = a_0 = 1$ for the scale factor at the present time, we have $\sinh y_0 = \sqrt{\Theta_{\Lambda 0}/\Theta_{k0}}$ and from $q = -\ddot{a}a/\dot{a}^2$, we find $\Theta_{k0} = -\Theta_{\Lambda 0}(1 + q_0)/q_0$.

We can determine the present age of the universe t_0 from the relation $H(t_0) = H_0$. We find

$$H_0 t_0 = \frac{1}{\sqrt{-q_0}} \text{atanh}(\sqrt{-q_0}) . \quad (2.20)$$

Of course, $\Theta_{\Lambda 0} + \Theta_{k0} = 1$, because the mass parameters are negligible in this approximation.

Figure 2 shows the solution $a(t)$ of equation (2.15) for three different z_{\max} (solid lines). The dashed lines show equation (2.19) with the same $H_0 t_0$ as the exact solutions; in other words, these approximated solutions have a different set of Θ 's but the same slope at t_0 of the exact solutions. Of course, at increasing z_{\max} the two solutions of equations (2.15) and (2.18) start to become indistinguishable at earlier and earlier times.

In the accelerated limit, we can analytically compute the luminosity distance $d_L = x(1 + z)$, where the radial distance x is implicitly defined by the relation

$$\int_0^x \frac{dr}{\sqrt{1 - kr^2}} = \int_{t_1}^{t_0} \frac{dt}{a(t)} \quad (2.21)$$

and t_1 is the time of the light emission. One finds

$$\int_{t_1}^{t_0} \frac{dt}{a(t)} = \frac{1}{\sqrt{\Theta_{k0}} H_0} \ln \left[\frac{\tanh(y_0/2)}{\tanh(y_1/2)} \right] \quad (2.22)$$

whereas

$$\int_0^x \frac{dr}{\sqrt{1 - kr^2}} = \frac{1}{\sqrt{-k}} \sinh^{-1}(\sqrt{-k}x) \quad (2.23)$$

with $k < 0$. With some algebra, we obtain

$$d_L = \frac{(1 + z)^2}{q_0 H_0} \left[\left(1 + q_0 - \frac{q_0}{(1 + z)^2} \right)^{1/2} - 1 \right] . \quad (2.24)$$

Because equation (2.19) is an excellent approximation to the exact solution of equation (2.15) at sufficiently late times, we can safely apply equation (2.24) to the real Universe and consider the distance modulus $m - M = \mu(z; q_0) = 25 + 5 \log_{10}[d_L(z; q_0)/\text{Mpc}]$, where q_0 is the only free parameter.

2.2 Kinematic Conformal Cosmology (KCG)

The starting point of KCG [35] is the static Schwarzschild solution of CG which yields the metric

$$ds^2 = -B(r)c^2 dt^2 + \frac{dr^2}{B(r)} + r^2 d\Omega \quad (2.25)$$

where

$$B(r) = 1 - \frac{\beta(2 - 3\beta\gamma)}{r} - 3\beta\gamma + \gamma r - \kappa r^2; \quad (2.26)$$

β and γ depend on the source mass and κ is a constant. If we consider sufficiently large distances from the mass source [$r \gg \beta(2 - 3\beta\gamma)$] and ignore the term $\beta\gamma$, that rotation velocities of spiral galaxies suggest to be negligible [39, 40], $B(r)$ simplifies to

$$B(r) = 1 + \gamma r - \kappa r^2. \quad (2.27)$$

By using the local conformal invariance, we can show that this metric is conformal to the standard FRW metric

$$ds^2 = -c^2 dt^2 + a^2(\mathbf{t}) \left(\frac{d\mathbf{r}^2}{1 - \mathbf{k}\mathbf{r}^2} + \mathbf{r}^2 d\Omega \right) \quad (2.28)$$

with $\mathbf{k} = k/|k| = 0, \pm 1$, and $k = -\gamma^2/4 - \kappa$. We omit the transformations between the coordinates (r, t) and the coordinates (\mathbf{r}, \mathbf{t}) which can be found in [35, 53].

The local conformal invariance introduces a dependence of the length and time units on the local metric. The redshift

$$1 + z = \frac{a(\mathbf{t}_0)}{a(\mathbf{t})} \quad (2.29)$$

can thus be interpreted as the ratio between the wavelength $\lambda(\mathbf{r}, \mathbf{t})$ of the radiation emitted by the atomic transitions at the time and location of the source and the wavelength $\lambda(0, \mathbf{t}_0)$ of the same atomic transitions measured on Earth now:

$$1 + z = \frac{\lambda(\mathbf{r}, \mathbf{t})}{\lambda(0, \mathbf{t}_0)}. \quad (2.30)$$

Unlike the standard cosmology, where the measured redshift is due to the expansion of the scale factor a , in KCG, the redshift originates from the change of length and time units over the cosmological time and space.

With this interpretation of the cosmic redshift, we can derive the dependence of the scale factor a on \mathbf{r} or \mathbf{t} without explicitly solving the field equations. In fact, $1 + z = \lambda(\mathbf{r}, \mathbf{t})/\lambda(0, \mathbf{t}_0)$ is the ratio of two frequencies $\nu(0, \mathbf{t}_0)/\nu(\mathbf{r}, \mathbf{t})$ which reduces to the ratio of two time intervals, or the square-root of the ratio of the time-time components g_{00} of the metric at the two different locations.

With the metric (2.25),

$$1 + z = \sqrt{\frac{-g_{00}(0, t_0)}{-g_{00}(r, t)}} = \frac{1}{\sqrt{1 + \gamma r - \kappa r^2}}, \quad (2.31)$$

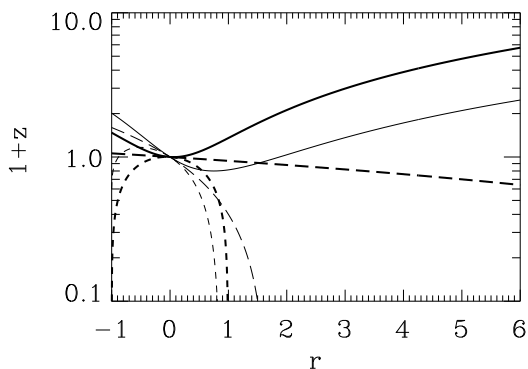


Figure 3. Relation between redshift z and radial coordinate \mathbf{r} of the FRW metric in KCG. The solid, long-dashed and short-dashed lines are for $\mathbf{k} = -1, 0$, and 1 , respectively. The bold (thin) lines are for $\delta = 0.06$ (0.6).

which yields, with the proper coordinate transformations to the metric (2.28),

$$1 + z = \frac{a(0)}{a(\mathbf{r})} = \sqrt{1 - \mathbf{k}\mathbf{r}^2} - \delta\mathbf{r} \quad (2.32)$$

where

$$\delta = \frac{\gamma}{2} \begin{cases} |k|^{-1/2} & k \neq 0 \\ 1 & k = 0. \end{cases}$$

Figure 3 shows the redshift $1 + z = a(0)/a(\mathbf{r})$ as a function of the radial coordinate \mathbf{r} . The origin of \mathbf{r} is our observer location, the coordinate \mathbf{r} indicates locations of sources whose radiation has already reached us (if $\mathbf{r} > 0$) or will reach us in the future (if $\mathbf{r} < 0$). Clearly, the observed redshift $z > 0$ appears only if $\mathbf{k} = -1$ when $\mathbf{r} > 0$. Therefore models with $\mathbf{k} = 0$ or 1 are not viable. The case $\mathbf{k} = -1$ also has a range of positive \mathbf{r} where $z < 0$; spectra of sources at these locations would be blueshifted. However, this range of \mathbf{r} decreases with decreasing δ and can be easily accommodated in the local neighborhood of the Solar System. Variaschi [48, 53] actually suggests that this feature provides a solution to the Pioneer anomaly [54].⁴ When $\mathbf{k} = -1$, equation (2.32) yields

$$\mathbf{r} = \frac{\delta(1 + z) \pm \sqrt{(1 + z)^2 - (1 - \delta^2)}}{1 - \delta^2} \quad (2.33)$$

and the two locations where $z = 0$ are $\mathbf{r} = 0$ and $\mathbf{r}_{\text{rs}} = 2\delta/(1 - \delta^2)$. There is also a minimum (negative) redshift at $\mathbf{r}_{\text{min}} = \delta/\sqrt{1 - \delta^2}$; \mathbf{r}_{min} is a real number only if $|\delta| < 1$.

To derive the luminosity distance d_L in KCG, we consider the following argument. The new interpretation of redshift implies that time (i.e. $1/\nu$) and length (i.e. λ) scale as

$$\Delta l_z = (1 + z)\Delta l_0 \quad (2.34)$$

$$\Delta t_z = (1 + z)\Delta t_0, \quad (2.35)$$

⁴More recent investigations seem to indicate that the measured anomalous acceleration of the Pioneer 10 and 11 spacecraft is not a gravitational effect but it rather is a thermal acceleration [e.g., 55] that might not even point to the Sun [56].

where the subscript 0 indicates units of the given quantity associated to objects which share the same location (in space and time) of the observer at the origin (namely us at $\mathbf{r} = 0$) and the subscript z indicates the same quantities associated to objects at redshift $z \neq 0$, measured by the same observer at the origin. For example, for an atomic transition that happens here we measure the frequency ν_0 ; for the same atomic transition that happens at redshift $z > 0$ we measure (here) the lower frequency $\nu_z = \nu_0/(1+z)$. It is important to emphasize that this frequency change is due to the different location in space and time of the atom and not to the cosmic expansion as in the standard model. The stretching of the space-time manifold also allows for a generic scaling of the mass:

$$\Delta m_z = f(1+z)\Delta m_0 \quad (2.36)$$

where $f(1+z)$ is an arbitrary function. Clearly, the energy $\Delta E \propto \Delta l^2 \Delta t^{-2} \Delta m$ scales with the same factor $f(1+z)$:

$$\Delta E_z = f(1+z)\Delta E_0. \quad (2.37)$$

According to these scaling laws, the relation between the luminosity L_z of a source at $z \neq 0$ and the luminosity L_0 of the same source located at $z = 0$ is

$$L_z = L_0 \frac{f(1+z)}{1+z}. \quad (2.38)$$

In other words, L_z is the luminosity we measure on Earth when the source is at position \mathbf{r} where the redshift is $z \neq 0$. In practice, we do measure the flux $F = L_z/4\pi d_L^2$, and not L_z . Classically, L_z is constant and the measured flux only depends on the distance d_L . In KCG, L_z is not constant, but depends on the location of the source and scales according to equation (2.38). To account for this scaling, Varieschi generalizes the definition of flux to $F \sim L_0/4\pi d^{a_V}$, where L_0 is now constant, because it is the luminosity of the source at $z = 0$, and the dependence of L_z on z enters the power a_V . Without a correction factor, the case $a_V \neq 2$ does not of course yield a quantity with the dimensions of a flux. Therefore, the proper generalization suggested by Varieschi is

$$F(d_L) = \frac{L_0}{4\pi d_L^2} \left(\frac{d_{rs}}{d_L} \right)^{a_V} \quad (2.39)$$

where d_{rs} is the luminosity distance of the source at $\mathbf{r} = \mathbf{r}_{rs}$ where $z = 0$. Of course $F(d_L) = L_z/4\pi d_L^2$ still holds. By combining this relation with equations (2.39) and (2.38) we determine the scaling function

$$\frac{f(1+z)}{1+z} = \left(\frac{d_{rs}}{d_L} \right)^{a_V}. \quad (2.40)$$

In standard cosmology, the energy per unit time received on Earth is dimmed by a factor $(1+z)^2$ because of the redshift of the photon frequency and the time interval dilation. This dimming originates a factor $(1+z)$ in the luminosity distance $d_L = a_0 x(1+z)$, where a_0 is the scale factor at the present time, and x is the radial coordinate of the FRW metric. In KCG, neither the energy nor the time are affected by the expansion of the scale factor. Therefore, the luminosity distance simply is

$$d_L = a(\mathbf{t}_0)\mathbf{r} \quad (2.41)$$

where the radial coordinate \mathbf{r} of the object at redshift z (equation 2.33) is evaluated by the observer at the origin, namely with $\delta = \delta(\mathbf{t}_0) \equiv \delta_0$. We thus have $d_{\text{rs}} = a(\mathbf{t}_0)2\delta_0/(1 - \delta_0^2)$ and

$$\frac{f(1+z)}{1+z} = \left[\frac{2\delta_0}{\delta_0(1+z) + \sqrt{(1+z)^2 - (1-\delta_0^2)}} \right]^{a_V}. \quad (2.42)$$

In the above equation we have used equation (2.33) with the positive sign, which is the solution for $z > 0$ and $\mathbf{r} > \mathbf{r}_{\text{rs}}$.

In standard cosmology, the distance measure $\mu = m - M = -2.5 \log_{10}[F(d_L)/F(d_{\text{ref}})] = 2.5(2 + a_V) \log_{10}(d_L/d_{\text{ref}})$ clearly has $a_V = 0$ and d_{ref} arbitrarily chosen to be $d_{\text{ref}} = 10$ pc. In KCG, a_V is unknown, and it is natural to choose $d_{\text{ref}} = d_{\text{rs}}$ where $z = 0$. We thus obtain

$$\begin{aligned} \mu(z) &= 2.5(2 + a_V) \times \\ &\times \log_{10} \left[\frac{\delta_0(1+z) + \sqrt{(1+z)^2 - (1-\delta_0^2)}}{2\delta_0} \right]. \end{aligned} \quad (2.43)$$

Obviously, this relation relies on the arbitrarily chosen equation (2.39) which leads to the definition of $f(1+z)$ (equation 2.42). Therefore, although this choice appears to provide a good description of the SN data, it might not necessarily be the final correct choice [53].

3 Bayesian analysis

We now apply the Bayesian analysis (see appendix A.1) to the GRB sample to derive the cosmological parameters of Λ CDM and of our two alternative models along with the coefficients of four GRB correlations. We also derive the cosmological parameters by applying the Bayesian analysis to a SN sample only and to the combined GRB and SN samples.

3.1 GRB sample

Among the distance indicators that correlate with the GRB luminosity $L = 4\pi d_L^2 P_{\text{bol}}$, where P_{bol} is the bolometric peak flux, we consider the following [21]:

- (1). τ_{lag} , the time delay between the soft and the hard light curve;
- (2). τ_{RT} , the minimum time over which the light curve rises by half the peak flux of the pulse;
- (3). V , the variability of the light curve defined in [21];
- (4). E_{peak} , the photon energy where the spectral energy distribution νF_ν peaks.

As we mention in the Introduction, we do not follow the inappropriate procedure of assuming a cosmological model, calibrating the relations, and deriving the GRB Hubble diagram. We instead apply the Bayesian analysis directly to the observables. Our GRB data set is $\{P_{\text{bol}}^i, \{Q^i\}_{j=1,4}, z^i, \mathbf{S}^i\}$, where $\{Q^i\}_{j=1,4} = \{\tau_{\text{lag}}^i, \tau_{\text{RT}}^i, V^i, E_{\text{peak}}^i\}$ and \mathbf{S}^i is the vector of uncertainties of all the measures, except for the redshift z^i .

Our task is the determination of the multi-dimensional PDF of the parameters $\theta = \{a, b, \sigma_{\text{int}}\}_{j=1,4}, \mathbf{p}\}$, where (a_j, b_j) are the parameters of the four GRB correlations. In the Λ CDM and CG models

$$\log_{10} P_{\text{bol}} = a_j + b_j \log_{10} Q_j - \log_{10}[4\pi d_L^2(z, \mathbf{p})]. \quad (3.1)$$

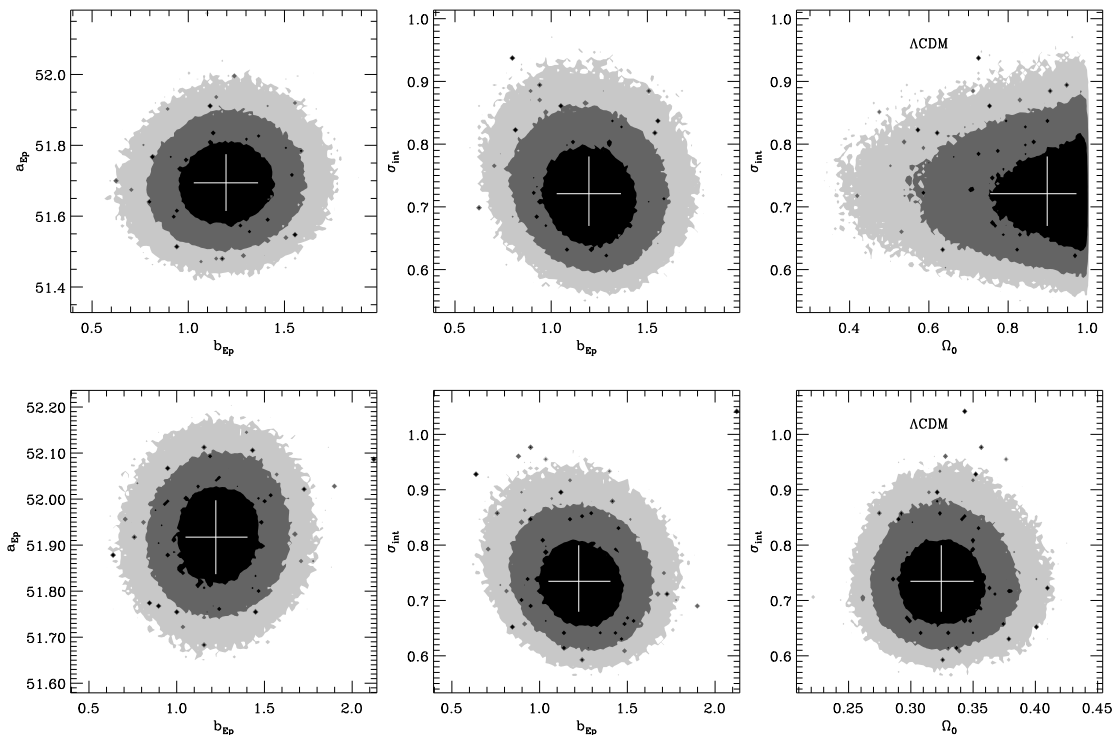


Figure 4. The marginalized PDFs of Ω_0 and of the parameters a , b , and σ_{int} of the $L - E_{\text{peak}}$ GRB correlation in the ΛCDM model. Black, grey, and light-grey shaded regions correspond to the 68.3, 95.4 and 99.7 percent confidence levels, respectively. The crosses show the median values and their marginalized $1\text{-}\sigma$ uncertainty. The top panels show the PDFs when the Bayesian analysis is applied to the GRB sample alone, the bottom panels show the PDFs when the GRB and SN samples are combined.

To mimic additional hidden parameters in the relations we assume that $\log_{10} P_{\text{bol}}^i$ is a random variate with mean

$$\log_{10} P_{\text{bol}} = a_j + b_j \log_{10} Q_j^i - \log_{10}[4\pi d_L^2(z^i, \mathbf{p})] \quad (3.2)$$

and variance σ_{int}^2 (e.g., [57], [58]); finally, \mathbf{p} is the vector of the cosmological parameters: in practice, $\mathbf{p} = \Omega_0$, with $\Omega_{\Lambda 0} = 1 - \Omega_0$ for ΛCDM ,⁵ and $\mathbf{p} = q_0$ for CG. For both ΛCDM and CG, the Hubble constant is an input parameter and we use $H_0 = 73 \pm 2(\text{statistical}) \pm 4(\text{systematic}) \text{ km s}^{-1} \text{ Mpc}^{-1}$ [60].

In KCG, the Hubble constant does not enter the estimate of d_L (equations 2.33 and 2.41). The flux measured on Earth of the source at redshift z , whose luminosity measured on Earth is $L_z = L_0 f(1+z)/(1+z)$, is

$$P(d_L) = \frac{L_0}{4\pi d_L^2} \left(\frac{d_{\text{rs}}}{d_L} \right)^{a_V}, \quad (3.3)$$

where $d_{\text{rs}} = a(t_0)2\delta_0/(1-\delta_0^2)$. Suppose the expected relation is between quantities associated to GRBs if they were at $z = 0$; in other words, suppose we expect relations of the form

⁵For the sake of simplifying the algorithm implementation, for the ΛCDM model, we use the analytic approximation to d_L in flat universes provided by Pen [59]. The formula is 0.4 percent accurate when Ω_0 is in the range [0.2, 1].

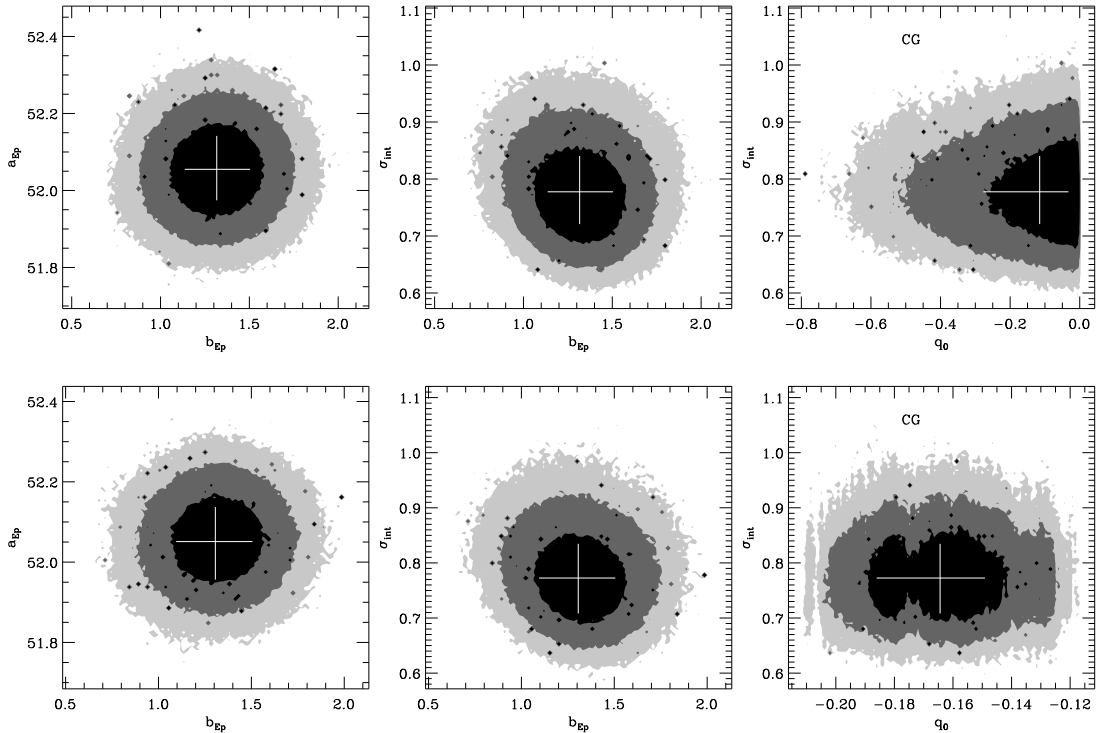


Figure 5. Same as figure 4 for the CG model.

$\log_{10} L_0 = a + b \log_{10} Q_0$. In this case, we have

$$\begin{aligned} \log_{10} P_{\text{bol}}(d_L) = & a_j + b_j \log_{10} Q_{0j} - \log_{10}(4\pi d_L^2) + \\ & - a_V \log_{10} \left(\frac{d_L}{d_{\text{rs}}} \right). \end{aligned} \quad (3.4)$$

Q_{0j} is either a time $\tau_0 = \tau_z/(1+z)$ or a frequency $E_0 = E_z(1+z)$.⁶ τ_z is the time of the source at redshift z measured on Earth and E_z is the frequency, measured on Earth, of the photons emitted at the source at redshift z . Finally, the cosmological parameters in KCG are $\mathbf{p} = [a_V, \delta_0, a(\mathbf{t}_0)]$.

We consider the 115 GRBs of Xiao and Schaefer [61]. The likelihood we assume for our Bayesian analysis is reported in appendix A.1. The analysis determines, at the same time, the cosmological parameters and the correlation coefficients. The top panels of figures 4, 5, and 6 show the marginalized PDFs of the correlation coefficients of the relation $L - E_{\text{peak}}$ and the cosmological parameters in our three models; in KCG we show the parameter δ_0 . The PDFs of the parameters of the remaining correlations are similar. The parameters of the four correlations are listed in Table 1 and the cosmological parameters are listed in Table 2. Figures 7, 8, and 9 show the four relations in the three models.

A visual inspection of these figures and the results in the tables show that all the three models have no difficulty in accommodating the current GRB data. In addition, our results

⁶For E_z , we use the frequency scaling relation rather than the energy relation $E_0 = E_z/f(1+z)$ discussed in section 2.2, because the X-ray photons originated in the GRBs of our sample are detected via photoelectric or Compton effects, and in these electron-photon interactions the electron is ultimately sensitive to the photon frequency.

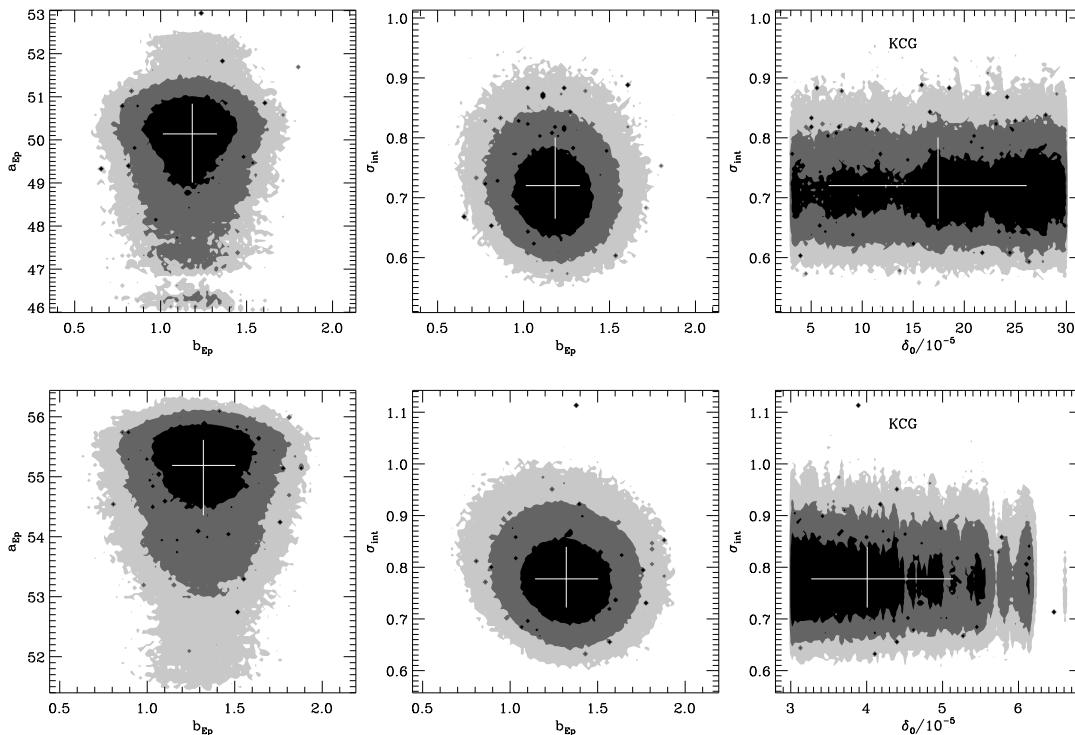


Figure 6. Same as figure 4 for the KCG model.

for Λ CDM are comparable to the relations shown in [61]. Our analysis also shows that, in Λ CDM, the GRBs imply $\Omega_0 = 0.90^{+0.07}_{-0.14}$ (Table 2), a factor three larger than other current measures.

3.2 SN sample

For the first time, in the section above, we have shown how the GRBs alone can be used to extract cosmological information without any prior information on the cosmological model and without any support from other observables. However, current measures of the GRB quantities are affected by large uncertainties and the cosmological constraints are consequently rather poor. To put more stringent constraints on the cosmological models, we can combine the GRBs with other cosmological probes. As an illustrative example we investigate the combination with SNe. Before doing so, we first apply our Bayesian analysis to the SN data alone.

SNe Ia are not exactly standard candles. In fact, we can not trivially estimate their distance moduli as $\mu = m^{\max} - M$, where m^{\max} is the apparent magnitude at the peak of the light curve in a given band and M an absolute magnitude valid for all SNe, because an empirical correlation between colour, magnitude at peak brightness, and shape of the light curve exists [62]. Instead, an appropriate procedure is to consider, for each i -th SN at redshift z_i , the following empirical distance modulus in the B band, which includes corrections due to the shape-parameter s of the light-curve and the color $c = B - V(t = B_{\max}) + 0.057$ [see, e.g., 63, 64]

$$\mu_i = m_i^{\max} - M + \alpha(s_i - 1) - \beta c_i . \quad (3.5)$$

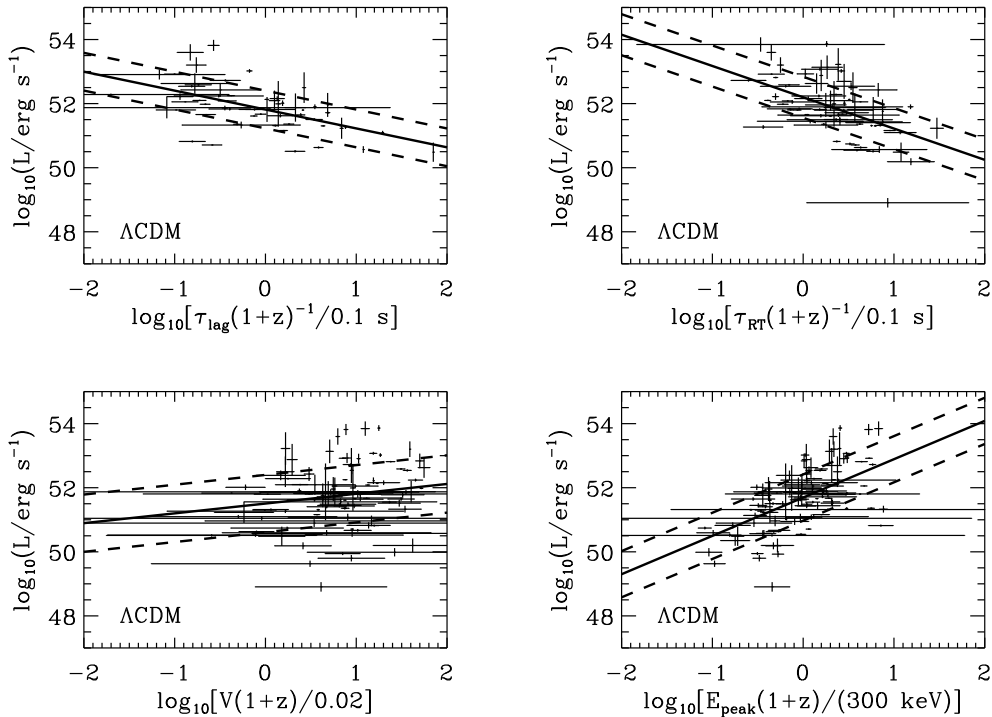


Figure 7. The four GRB correlations when the Bayesian analysis is applied to the GRB sample alone in the Λ CDM model. The crosses show the GRB measurements with the $1\text{-}\sigma$ errorbars. The thick solid straight-lines are the correlations according to the coefficients listed in Table 1. The dashed lines show the $\pm\sigma_{\text{int}}$ standard deviation of each relation.

To estimate the three parameters M , α , and β along with the cosmological parameters \mathbf{p} , we apply the Bayesian analysis to the data sample $\{m_i, s_i, c_i, z_i, \mathbf{S}_i\}$, where \mathbf{S}_i is the vector of the uncertainties of the four observables of each SN. As in the previous section, additional hidden parameters are mimicked in the relation between the observable m^{max} and μ , by assuming that m^{max} is a random variate with mean

$$m(\mathbf{p}) = \mu(\mathbf{p}, z_i) + M - \alpha(s_i - 1) + \beta c_i \quad (3.6)$$

and variance σ_{int}^2 .

Whereas for Λ CDM and CG, $\mathbf{p} = \Omega_0$ and $\mathbf{p} = q_0$, respectively, as in the GRB analysis, for KCG, $\mathbf{p} = (a, \delta_0)$ and the number of parameters is reduced by one. In the Λ CDM and CG models the expected distance modulus is $\mu = 25 + 5 \log(d_L/\text{Mpc})$, where d_L is given by equation (2.24) for CG. In the KCG model, μ is given instead by equation (2.43). Therefore, in this latter model the value of H_0 is irrelevant, whereas for Λ CDM and CG, μ also depends on the Hubble constant through d_L . We follow the usual procedure of removing the value of H_0 and its uncertainty by replacing M with $M' = M - 5 \log(H_0)$.

The likelihood we assume for our Bayesian analysis is reported in appendix A.1. We determine, at the same time, the cosmological parameters, the absolute magnitude M of the SNe and the SN parameters α and β , which, in turn, can be used to compute the distance moduli of the SNe.

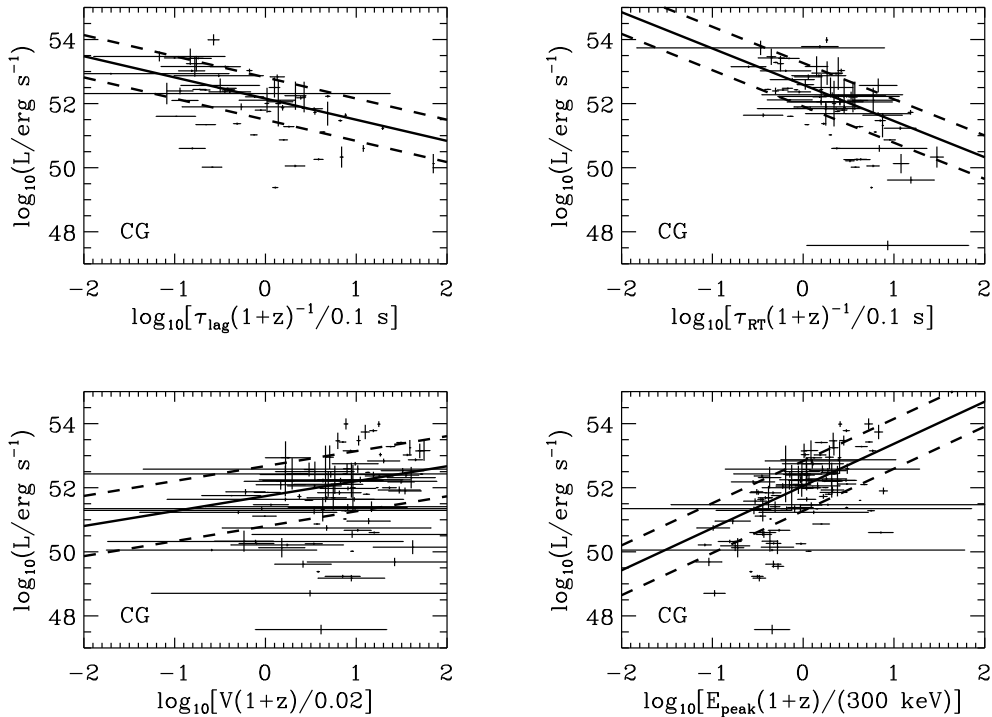


Figure 8. Same as figure 7 for the CG model.

We consider the 397 SNe of the Constitution set [65]. Figures 10-11 and Table 3 show our results. All the three models provide the same pair (α, β) within the confidence levels; Λ CDM and CG also provide the same effective absolute magnitude M , which is fully consistent with the absolute magnitudes of nearby SNe [66]. Previous estimates of both Ω_0 for Λ CDM (e.g., $\Omega_0 = 0.29 \pm 0.01$ by [67]) and q_0 for CG ($q_0 = -0.37$ by [13]) are largely within $3\text{-}\sigma$ of our estimates $\Omega_0 = 0.312^{+0.024}_{-0.023}$ and $q_0 = -0.225^{+0.068}_{-0.066}$, respectively. We note that the reference value of Ω_0 we mention was determined by combining SNe with other probes, whereas our estimate of Ω_0 and Mannheim’s and our estimates of q_0 rely on SNe alone. In addition, the analysis of [67], unlike ours, include the covariance matrix of each SN: based on the comparable results we obtain, we do not expect that our approach substantially suffers from this simplification.

In KCG, the absolute magnitudes of nearby SNe also appear to be within $2\text{-}\sigma$ of our estimate $M = -16.0^{+2.5}_{-2.0}$; moreover $\delta_0 = 3.83 \times 10^{-5}$, which was estimated by Varieschi [53] by keeping $a_V = 2$ fixed, is within $2\text{-}\sigma$ of our median value $\delta_0 = 7.8^{+6.0}_{-2.8} \times 10^{-5}$. However, the parameter M cannot be directly compared to the absolute magnitudes of nearby SNe which were estimated in a cosmological framework based on fundamentally different physical principles. In addition, the 68.3 percent confidence intervals are large (~ 15 percent for M and ~ 60 percent for δ_0) because M and δ_0 are more strongly degenerate than M and Ω_0 or q_0 in the other models (figure 10). At any rate, the most important result of our analysis of KCG, that we clearly see in the right panel of figure 11, is that the data are consistent with a SN Hubble diagram substantially different from what it is naively assumed to be a *measured* Hubble diagram: the distance moduli of SNe in this model are ~ 3 mag fainter

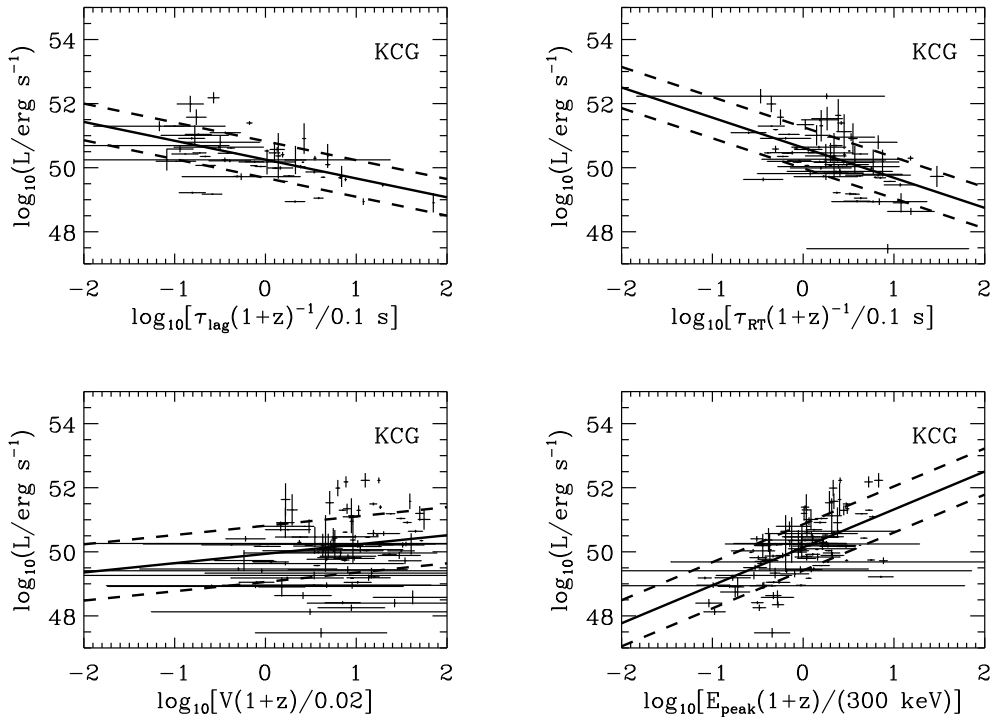


Figure 9. Same as figure 7 for the KCG model.

than in Λ CDM. The reason for this result is simple: the SN apparent magnitudes are the direct observables, whereas the SN distance moduli are not. So, if KCG were the widely accepted standard cosmological model, and we tested Λ CDM by assuming that the distance moduli are the direct observables, Λ CDM would be completely unable to describe the data. Clearly our approach easily prevents us from drawing this incorrect conclusion.

From figures 10-11 and Table 3, we conclude that the three models describe the SN data very well. Our result shows that SNe alone do not necessarily support an early phase of decelerated expansion, but are consistent with an always accelerating universe. Amendola et al. [68] show that the SN data are consistent with a universe where the transition between the decelerated and the accelerated phase can occur as early as $z \sim 3$. Our analysis suggests the more extreme conclusion that the current SN data are consistent with models where the transition phase never occurred.

3.3 GRBs combined with SNe

In the Bayesian approach, combining the SN and GRB samples simply translates into considering a single sample $S = \{\text{SN}_i, \text{GRB}_j\}$, where $\text{SN}_i = \{m_i, s_i, c_i, z_i\}$, with corresponding uncertainties \mathbf{S}_i , and $\text{GRB}_j = \{P_{\text{bol}}^j, Q_j^i, z_j\}$, with $Q_j = \{\tau_{\text{lag}}^i, \tau_{\text{RT}}^i, V^i, E_{\text{peak}}^i\}$ and corresponding uncertainties \mathbf{S}_i . As usual, our task is the determination of the multi-dimensional probability density distribution of the parameters $\theta = \{\alpha, \beta, M, \sigma_{\text{int}}^{\text{SN}}, \{a, b, \sigma_{\text{int}}\}_j, \mathbf{p}\}$, where $\{a, b, \sigma_{\text{int}}\}_j, j = 1, 4$, are the parameters of the four GRB correlations.

The bottom panels of figures 4, 5, and 6 show the marginalized PDFs of the correlation coefficients of the relation $L - E_{\text{peak}}$ and the cosmological parameters in our three models

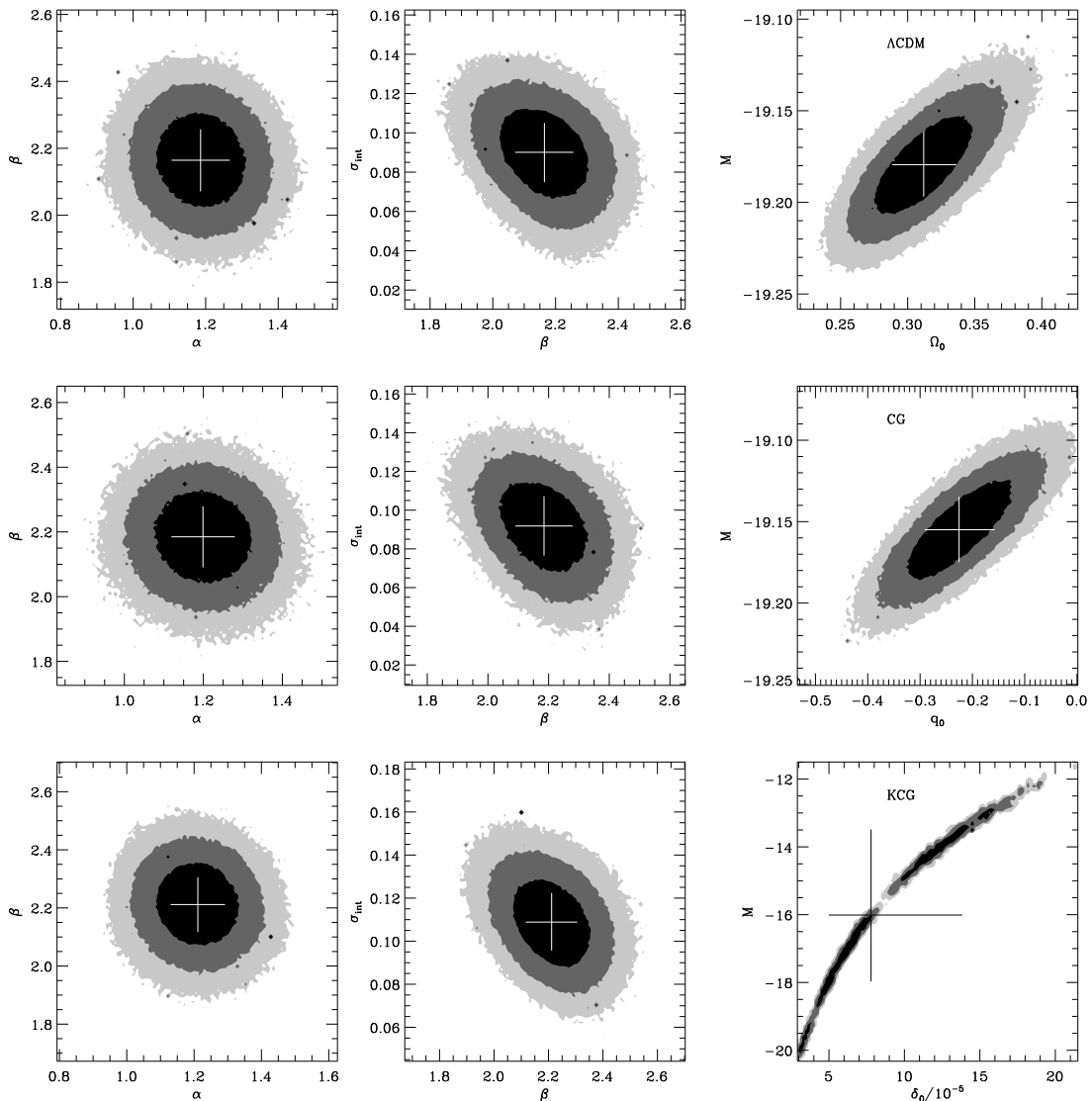


Figure 10. The marginalized PDFs of the cosmological parameters of our three models and of the SN parameters in equation (3.5) when the Bayes analysis is applied to the SN sample alone: Λ CDM (upper row), CG (middle row), KCG (bottom row). Black, grey, and light-grey shaded regions correspond to the 68.3, 95.4, and 99.7 percent confidence levels, respectively. The crosses show the median values and their marginalized $1\text{-}\sigma$ uncertainty.

obtained when we combine the GRB and SN samples. Both the SN parameters (Table 3) and the GRB correlation parameters (Table 1) are barely affected by this combination. On the contrary, the cosmological parameters are closer to the values obtained with the SN sample alone than to the values obtained with the GRBs alone. Clearly, this is a consequence of the fact that the SN sample is larger and the uncertainties on the SN measurements smaller. As it happened with the SNe and the GRBs analysed separately, the three models describe the data properly.

We also plot the Hubble diagrams of GRBs in our three models (figure 12), for the sake of clarity and to make our results more easily comparable to previous results in the literature.

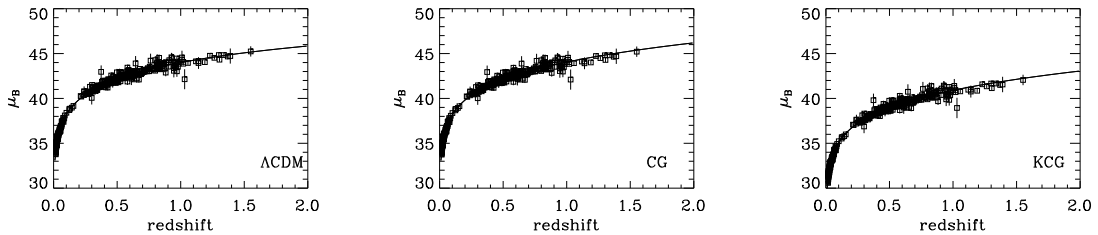


Figure 11. SN Hubble diagrams derived with equation (3.5) and the median fit parameters in our three models. The error bars are computed by considering only the uncertainties on m , s , and c . The solid curves show the $\mu - z$ relation computed with the corresponding median fit cosmological parameters.

To do so, we follow the standard approach [21] and for each i -th GRB we compute $\mu_i^{(j)}$ where j refers to one of the four relations: the directly observed quantity Q provides an estimate of $\log_{10} L = a + b \log_{10} Q$, which, in turns, returns d_L and thus $\mu_i^{(j)} = 5 \log_{10}(d_L/\text{Mpc}) + 25$ or $\mu_i^{(j)} = 2.5(2 + a_V) \log_{10}(d_L/d_{\text{rs}})$ for the KCG model. The final distance modulus is the weighted mean $\mu_i = \sum_{j=1}^4 w_j \mu_i^{(j)} / \sum_{j=1}^4 w_j$ where $w_j = 1/\sigma_j^2$ and σ_j^2 is the variance on $\mu_i^{(j)}$ derived with the usual error propagation law. Clearly, $\sigma_{\mu_i} = (\sum_{j=1}^4 w_j)^{-1/2}$ is the uncertainty on μ_i . Figure 12 shows the Hubble diagram when the parameters are derived from the analysis of the GRBs alone (upper panels) and when the SNe are included (lower panels). In ΛCDM and CG, the inclusion of the SNe has no visible effect. On the contrary, in the KCG model, the effect of the SNe is dramatic: they increase the distance moduli of GRBs by 50 percent. The solid curves are the distance moduli expected with the cosmological parameters derived from the Bayesian analysis. For ΛCDM our results are similar to the results of [21]. However, as mentioned above, both CG and KCG perform equally well, provided that the analysis of the data is done properly. Our result clearly shows that if we naively test alternative cosmological models by using GRB Hubble diagrams like those shown in figure 12 as they were direct measures, we can draw grossly incorrect conclusions.

4 Discussion

The Bayesian analysis described above shows that current data from SNe and GRBs can be easily described by both ΛCDM , that requires a deceleration/acceleration transition in the expansion of the Universe, and conformal gravity, that requires an always accelerating universe.

To understand quantitatively which model the GRB and SN data might favour, we compute the Bayes factor B_{12} defined in equation (A.12). We assume flat priors for all the parameters of the models but the internal dispersions, as explained in Appendix A.1. When we consider the GRB sample alone, we find that ΛCDM is favoured over CG by a factor $\ln B_{12} = 37.9$, and over KCG by a factor $\ln B_{12} = 12.0$ (Table 4). When we consider the SN sample alone, our Bayes factor estimate shows that ΛCDM is favoured over CG and KCG by a Bayes factor $\ln B_{12} = 6.6$ and $\ln B_{12} = 7.2$, respectively. Finally, for the SN and GRB sample combined, the Bayes factor again shows that ΛCDM is favoured, by a factor $\ln B_{12} = 1.5$ over CG and by a factor $\ln B_{12} = 24.3$ over KCG. According to Jeffreys' table

relation	N_{GRB}	model	a	b	σ_{int}
$L - \tau_{\text{lag}}$	59	ΛCDM	$51.815^{+0.094}_{-0.088}$	$-0.59^{+0.13}_{-0.13}$	$0.589^{+0.069}_{-0.060}$
			$52.042^{+0.085}_{-0.091}$	$-0.61^{+0.14}_{-0.14}$	$0.609^{+0.078}_{-0.060}$
		CG	$52.157^{+0.099}_{-0.095}$	$-0.66^{+0.15}_{-0.14}$	$0.661^{+0.078}_{-0.064}$
			$52.170^{+0.091}_{-0.099}$	$-0.68^{+0.15}_{-0.18}$	$0.67^{+0.10}_{-0.07}$
		KCG	$50.3^{+0.7}_{-1.1}$	$-0.59^{+0.14}_{-0.15}$	$0.571^{+0.073}_{-0.063}$
			$55.28^{+0.44}_{-0.85}$	$-0.66^{+0.14}_{-0.14}$	$0.664^{+0.075}_{-0.066}$
$L - \tau_{\text{RT}}$	79	ΛCDM	$52.12^{+0.10}_{-0.10}$	$-0.98^{+0.15}_{-0.16}$	$0.640^{+0.068}_{-0.057}$
			$52.44^{+0.10}_{-0.10}$	$-1.03^{+0.16}_{-0.17}$	$0.651^{+0.072}_{-0.061}$
		CG	$52.59^{+0.11}_{-0.11}$	$-1.13^{+0.17}_{-0.17}$	$0.678^{+0.071}_{-0.061}$
			$52.60^{+0.10}_{-0.10}$	$-1.12^{+0.18}_{-0.18}$	$0.684^{+0.081}_{-0.066}$
		KCG	$50.6^{+0.7}_{-1.1}$	$-0.94^{+0.18}_{-0.17}$	$0.643^{+0.079}_{-0.060}$
			$55.72^{+0.43}_{-0.84}$	$-1.14^{+0.17}_{-0.18}$	$0.677^{+0.070}_{-0.061}$
$L - V$	104	ΛCDM	$51.50^{+0.16}_{-0.15}$	$0.31^{+0.17}_{-0.17}$	$0.894^{+0.076}_{-0.069}$
			$51.70^{+0.16}_{-0.16}$	$0.34^{+0.19}_{-0.17}$	$0.908^{+0.079}_{-0.074}$
		CG	$51.74^{+0.18}_{-0.17}$	$0.47^{+0.19}_{-0.19}$	$0.939^{+0.083}_{-0.074}$
			$51.75^{+0.16}_{-0.17}$	$0.44^{+0.20}_{-0.16}$	$0.941^{+0.073}_{-0.075}$
		KCG	$49.9^{+0.7}_{-1.1}$	$0.29^{+0.18}_{-0.18}$	$0.877^{+0.079}_{-0.069}$
			$54.87^{+0.45}_{-0.86}$	$0.46^{+0.19}_{-0.20}$	$0.937^{+0.087}_{-0.072}$
$L - E_{\text{peak}}$	115	ΛCDM	$51.694^{+0.081}_{-0.079}$	$1.20^{+0.17}_{-0.17}$	$0.721^{+0.059}_{-0.051}$
			$51.917^{+0.080}_{-0.080}$	$1.22^{+0.18}_{-0.17}$	$0.735^{+0.065}_{-0.055}$
		CG	$52.055^{+0.087}_{-0.080}$	$1.32^{+0.19}_{-0.18}$	$0.778^{+0.063}_{-0.057}$
			$52.051^{+0.086}_{-0.095}$	$1.31^{+0.20}_{-0.21}$	$0.773^{+0.062}_{-0.064}$
		KCG	$50.1^{+0.7}_{-1.1}$	$1.18^{+0.14}_{-0.17}$	$0.720^{+0.080}_{-0.055}$
			$55.19^{+0.43}_{-0.83}$	$1.32^{+0.18}_{-0.18}$	$0.777^{+0.062}_{-0.055}$

Table 1. Median fit parameters of the GRB relations obtained from the analysis of the GRBs alone (first row of each model) and from the analysis of the GRBs and SNe combined (second row of each model). The uncertainties are the marginalized 68.3 percent confidence intervals. The second column lists the number of GRBs used for the estimate of each correlation.

[69],⁷ in most cases these values are large and ΛCDM would be “decisively” favoured over CG and KCG.

However, we emphasize that this conclusion is not as robust as it might appear. There is in fact an extended literature on how the Bayes factor is sensitive to the choice of the priors [e.g., 71–76]. Investigating this issue is beyond the scope of this work, but it is clear that different prior choices might substantially change our Bayes factor estimates and, consequently, the conclusion they suggest.

Overall, our analysis shows that GRBs are substantially unable to distinguish between

⁷Jeffreys [69] separates the values of the Bayes factor B_{12} into the six intervals [(< 1) , $(1, 3)$, $(3, 10)$, $(10, 30)$, $(30, 100)$, (> 100)], where larger B_{12} values favour model M_1 over model M_2 more strongly. It became customary to indicate the intervals in natural logarithms [(< 0) , $(1, 1.1)$, $(1.1, 2.3)$, $(2.3, 3.4)$, $(3.4, 4.6)$, (> 4.6)]. The choice of these intervals clearly is arbitrary and other, albeit comparable, choices were also adopted [e.g., 70].

model	\mathbf{p}		
Λ CDM	Ω_0		$0.90^{+0.07}_{-0.14}$ $0.324^{+0.026}_{-0.025}$
CG	q_0		$-0.12^{+0.08}_{-0.16}$ $-0.164^{+0.015}_{-0.022}$
KCG	$\delta_0/10^{-5}$, a_V , $a(\mathbf{t}_0)$	17^{+9}_{-11} , $4.0^{+1.1}_{-0.7}$	$1.035^{+0.066}_{-0.025}$, $2.038^{+0.013}_{-0.013}$, $5.5^{+3.3}_{-4.0}$, $5.3^{+3.0}_{-3.3}$

Table 2. Median fit cosmological parameters of the GRB relations obtained from the analysis of the GRBs alone (first row of each model) and from the analysis of the GRBs and SNe combined (second row of each model). The uncertainties are the marginalized 68.3 percent confidence intervals.

model	α	β	M	σ_{int}	\mathbf{p}		
Λ CDM	$1.186^{+0.081}_{-0.080}$ $1.182^{+0.088}_{-0.082}$	$2.164^{+0.092}_{-0.093}$ $2.153^{+0.097}_{-0.092}$	$-19.179^{+0.018}_{-0.017}$ $-19.172^{+0.019}_{-0.018}$	$0.090^{+0.015}_{-0.015}$ $0.0917^{+0.017}_{-0.016}$	Ω_0		$0.312^{+0.024}_{-0.023}$ $0.324^{+0.026}_{-0.025}$
CG	$1.199^{+0.081}_{-0.080}$ $1.193^{+0.098}_{-0.091}$	$2.185^{+0.094}_{-0.095}$ $2.18^{+0.12}_{-0.10}$	$-19.155^{+0.020}_{-0.020}$ $-19.142^{+0.014}_{-0.017}$	$0.0918^{+0.015}_{-0.015}$ $0.092^{+0.016}_{-0.017}$	q_0		$-0.225^{+0.068}_{-0.066}$ $-0.164^{+0.015}_{-0.022}$
KCG	$1.211^{+0.081}_{-0.081}$ $1.204^{+0.082}_{-0.084}$	$2.212^{+0.094}_{-0.095}$ $2.21^{+0.10}_{-0.10}$	$-16.0^{+2.5}_{-2.0}$ $-18.9^{+1.1}_{-0.9}$	$0.109^{+0.014}_{-0.013}$ $0.110^{+0.014}_{-0.013}$	$\delta_0/10^{-5}$, a_V	$7.8^{+6.0}_{-2.8}$, $4.0^{+1.1}_{-0.7}$	$2.044^{+0.013}_{-0.013}$, $2.038^{+0.013}_{-0.013}$

Table 3. Median fit parameters of the SN data alone (first row of each model) and when combined with the GRBs (second row of each model). The uncertainties are the marginalized 68.3 percent confidence intervals.

sample	Λ CDM/CG	Λ CDM/KCG
GRBs	37.9	12.0
SNe	6.6	7.2
GRBs+SNe	1.5	24.3

Table 4. Values of $\ln B_{12}$, where B_{12} is the Bayes factor in equation (A.12): $B_{12} > 1$ favours model M_1 over model M_2 .

two cosmological models that have very distinct predictions on the early expansion history of the Universe, where the GRBs are expected to provide unambiguous results. This failure is mostly due to the very large uncertainties on the GRB observables. In fact, our results obtained by combining GRBs with SNe confirm that the cosmological constraints are actually driven by the SNe rather than the GRBs [77]. Furthermore, GRB afterglow energies corrected for beaming span two orders of magnitude [78, 79], and current detectors can introduce significant bias against hard bursts in GRB samples [80]. It thus seems difficult to consider GRBs as standard candles, unless we are able to correct for these systematic effects, which appear to be substantial. We necessarily conclude that GRBs do not represent effective cosmological probes. Currently, enlarging the SN sample at $z > 1$ might remain a more promising method to constrain the expansion history of the Universe.

Additional tests of conformal gravity might come from the Bayesian analysis of the

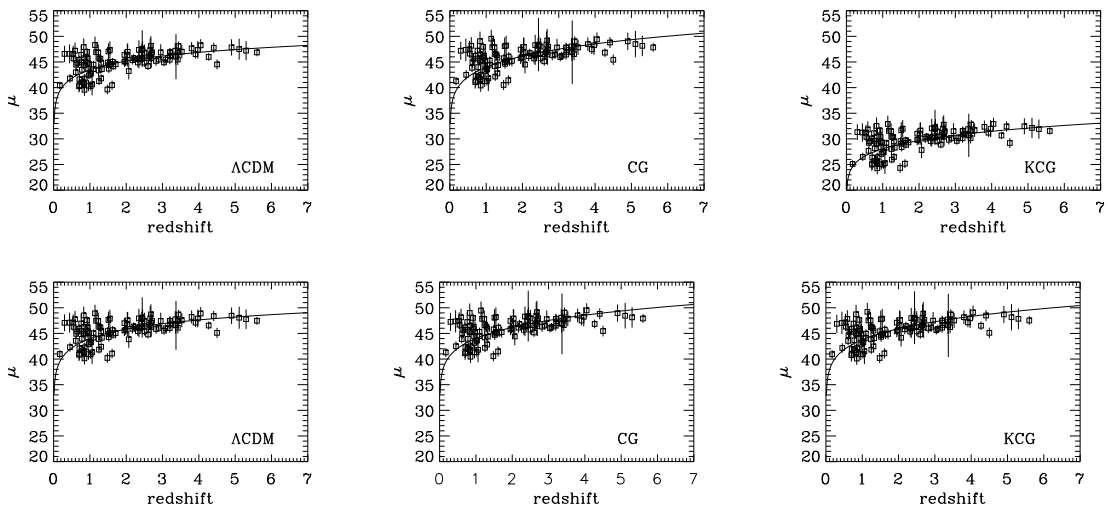


Figure 12. GRB Hubble diagrams based on the GRB data alone (upper panels) and on the sample of GRBs and SNe combined (lower panels). The solid curves are not fits to the data points, but the theoretical distance modulus of each model with the parameters derived with the Bayesian analysis.

combination of different cosmological probes deriving from both the expansion history of the Universe and the properties of cosmic structures. CG seems to have difficulties in describing the thermodynamics of clusters of galaxies [81, 82], whereas no investigation of structure formation in KCG is available yet. However, conformal gravity remains worth investigating for the elegant solution it suggests to the cosmological constant, zero-point energy and quantum gravity problems without resorting to either dark matter or dark energy [43, 83].

The additional merit of the models that largely depart from Λ CDM, like CG and KCG, is that they provide predictions that are clearly distinct from the standard model expectations. Our results teach us that we do need a proper technique to test the data against different models: using a method that partly relies on the models we want to test does not generally yield sensible results, unless the models are very similar to each other. In this case however, the conclusions we draw are weak. Using a really model-independent technique returns results that are definitely more robust. For example, we show that KCG, where the SN distance moduli are ~ 3 mag fainter than in Λ CDM, also can describe the data. We thus confirm that with the Bayesian technique we can robustly and self-consistently test various cosmological models, no matter how different they are.

5 Conclusion

Current data from SNe and, more recently, from GRBs are usually interpreted as supporting evidence for the Λ CDM model, where the expansion history of the Universe has an early deceleration phase, down to $z \sim 1$, followed by the acceleration phase that lasts to the present time. Based on this supposedly robust interpretation of the available data, most alternative cosmological models were conceived to reproduce these two distinct phases. On the contrary, conformal gravity was proposed well before the observation of high- z SNe and it predicts a Universe expansion that has been always accelerating. This model is thus ideal to test whether the data undoubtedly support Λ CDM.

We perform our test with two variants of conformal gravity: CG and KCG. KCG is an even more drastic alternative model than CG, because a number of physical quantities, including the flux from distant sources and the cosmological redshift, have a radically different interpretation than in the standard model. Therefore, unlike many cosmological tests described in the literature, ours requires a method that does not rely on any prior information from the same model that has to be tested.

We lay out the problem within a full Bayesian context, and perform three different analyses of a sample of GRBs, a sample of SNe and the sample of the GRBs and SNe combined. With our Bayesian approach, we simultaneously estimate the PDFs of the parameters of the GRB correlations, the parameters of the SN distance moduli and the cosmological parameters.

Contrary to the expectation, we show that the current data can be described by CG, KCG, and Λ CDM equally well. The application of our method to the SN sample alone shows that the data even support the SN distance moduli derived in KCG, where their physical interpretation is fundamentally different from Λ CDM, and are ~ 3 mag fainter than in the standard model. Similarly, the cosmological information that can be derived from the GRBs does also support CG and KCG when the information is extracted properly.

We conclude that, at face value, the Λ CDM expansion history is not supported by the data as robustly as it is naively believed, but other wildly different models can still describe the data satisfactorily. Therefore, current data are unable to exclude that the Universe has been always accelerating: both variants of conformal gravity we have investigated here are, from the point of view of the background expansion history of the Universe, viable alternatives to Λ CDM.

Λ CDM is favoured over CG and KCG only when we resort to the Bayes factor computed by assuming flat priors on the model parameters. It will be crucial to investigate whether Λ CDM still remains favoured for different choices of the priors or, more interestingly, when we include additional cosmological probes based on the formation of large-scale structure. In this context, Λ CDM requires large amounts of dark matter that is expected to be unnecessary in conformal gravity.

Acknowledgments

We sincerely thank Johannes Buchner and Michael Gruberbauer for developing their superb code APEMoST and making it available to the community (apemost.sourceforge.net). We also are particularly grateful to Johannes Buchner and Stefano Andreon for intense and enlightening correspondence on Bayesian statistics. Stefano Andreon is also acknowledged for a very stimulating seminar, delivered in Torino, on Bayesian statistics applied to astrophysics that inspired this work. We finally thank Margaret Geller, Xiao-Li Meng and the JCAP Editor, Carl Akerlof, for valuable suggestions on the presentation of our results. Support from the INFN grant PD51 and the PRIN-MIUR-2008 grant 2008NR3EBK_003 “Matter-antimatter asymmetry, dark matter and dark energy in the LHC era” is gratefully acknowledged. LO also acknowledges support from a 2009 National Fellowship “LORÉAL Italia Per le Donne e la Scienza” of the LORÉAL-UNESCO program For Women in Science and partial support from the ASI Contract No. I/016/07/0 COFIS. This research has made use of NASA’s Astrophysics Data System.

A Bayesian analysis

A.1 Bayesian parameter estimation

Consider a model M described by a set of parameters θ with probability $p(\theta|M)$ of occurring. The probability of measuring the set of data D when the model M is described by the parameters θ is the likelihood $p(D|\theta, M)$. The probability of observing a set of data D is thus

$$p(D|M) = \int p(D|\theta, M)p(\theta|M)d\theta ; \quad (\text{A.1})$$

$p(D|M)$ is called the Bayesian evidence of the model M , $p(\theta|M)$ the prior. We are interested in estimating the PDF of the parameters given our data set D

$$p(\theta|D, M) = \frac{p(D|\theta, M)p(\theta|M)}{p(D|M)}. \quad (\text{A.2})$$

For this task, we need to assume a likelihood $p(D|\theta, M)$.

For the GRBs, $D = \{P_{\text{bol}}^i, \{Q_j^i\}_{j=1,4}, z^i, \mathbf{S}^i\}$, $\{Q_j^i\}_{j=1,4} = \{\tau_{\text{lag}}^i, \tau_{\text{RT}}^i, V^i, E_{\text{peak}}^i\}$, \mathbf{S}^i is the vector of the uncertainties of $\{P_{\text{bol}}^i, \{Q_j^i\}_{j=1,4}\}$, $\theta = \{\{a_j, b_j, \sigma_{\text{int}_j}\}_{j=1,4}, \mathbf{p}\}$, \mathbf{p} is the vector of the cosmological parameters, and we assume the likelihood

$$p(D|\theta, M) = \prod_{j=1}^4 \prod_i \frac{1}{(2\pi\sigma_{ij}^2)^{1/2}} \exp\left[\frac{-(P_{\text{bol}}^i - W_j^i)^2}{2\sigma_{ij}^2}\right] \quad (\text{A.3})$$

where

$$\sigma_{ij}^2 = \sigma_{\text{int}_j}^2 + \sigma_{P_{\text{bol}}^i}^2 + b_j^2\sigma_{Q_j^i}^2 \quad (\text{A.4})$$

and

$$W_j^i = a_j + b_j Q_j^i - f(z^i; \mathbf{p}) \quad j = 1, \dots, 4 \quad (\text{A.5})$$

where $f(z^i; \mathbf{p})$ is the proper function of the luminosity distance d_L . W_j^i is the mean of the random variate $\log_{10} P_{\text{bol}}^i$, whose variance is $\sigma_{\text{int}_j}^2$, according to the j -th correlation.

For the SNe, $D = \{m_i, s_i, c_i, z_i, \mathbf{S}_i\}$, where \mathbf{S}_i is the vector of the observable uncertainties. If $\mu(z_i; \mathbf{p})$ is the distance modulus, and m_i a random variate with mean

$$W_i = \mu(z_i; \mathbf{p}) + M - \alpha(s_i - 1) + \beta c_i \quad (\text{A.6})$$

and variance σ_{int}^2 , the complete set of parameters is $\theta = \{M, \alpha, \beta, \sigma_{\text{int}}, \mathbf{p}\}$. We assume the likelihood

$$p(D|\theta, M) = \prod_i \frac{1}{(2\pi\sigma_i^2)^{1/2}} \exp\left[\frac{-(m_i - W_i)^2}{2\sigma_i^2}\right] \quad (\text{A.7})$$

where

$$\sigma_i^2 = \sigma_{\text{int}}^2 + \sigma_{m_i}^2 + \alpha^2\sigma_{s_i}^2 + \beta^2\sigma_{c_i}^2 + \sigma_{\mu_i}^2 ; \quad (\text{A.8})$$

$\sigma_{m_i}, \sigma_{s_i}, \sigma_{c_i}$ are the uncertainties of the observables and σ_{μ_i} derives from the uncertainty σ_{z_i} on the SN redshift z_i .

For both the SN and GRB samples, we assume independent flat priors for all the θ parameters except for the internal dispersions σ_{int} , which are positive defined. In this case we assume

$$p(\sigma_{\text{int}}|M) = \frac{\mu^r}{\Gamma(r)} x^{r-1} \exp(-\mu x) \quad (\text{A.9})$$

where $x = 1/\sigma_{\text{int}}^2$, and $\Gamma(r)$ is the usual gamma function. This PDF describes a variate with mean r/μ , and variance r/μ^2 . We set $r = \mu = 10^{-5}$ to assure an almost flat prior.

A.2 Bayesian model selection

The probability of the model M to be correct, given the set of data D is, according to Bayes' theorem, the model posterior probability

$$p(M|D) = \frac{p(D|M)p(M)}{p(D)}. \quad (\text{A.10})$$

When comparing two models M_1 and M_2 , we can compute the ratio of the posterior probabilities

$$\frac{p(M_1|D)}{p(M_2|D)} = B_{12} \frac{p(M_1)}{p(M_2)} \quad (\text{A.11})$$

where

$$B_{12} = \frac{p(D|M_1)}{p(D|M_2)} \quad (\text{A.12})$$

is the Bayes factor. If $p(M_1) = p(M_2)$, $B_{12} > 1$ clearly favours model M_1 ; M_2 is favoured otherwise. Estimating the Bayesian evidence $p(D|M)$ of a model thus provides a tool to compare different models for a given set of data, if the models are equally probable.

The computation of the Bayesian evidence is not a trivial task [see, e.g., 84, for a review]. We use here the thermodynamic integration (or parallel tempering; [e.g., 85]). The posterior probability for the model parameters is

$$p(\theta|D, M) = \frac{p(D|\theta, M)p(\theta|M)}{p(D|M)}. \quad (\text{A.13})$$

The evidence $p(D|M)$ is a normalization constant; we can thus define the unnormalized probability density

$$q(\theta|D, M) = p(D|\theta, M)p(\theta|M). \quad (\text{A.14})$$

Consider the variant

$$q_\beta(\theta|D, M) = [p(D|\theta, M)]^\beta p(\theta|M) \quad (\text{A.15})$$

and

$$p_\beta(\theta|D, M) = \frac{[p(D|\theta, M)]^\beta p(\theta|M)}{p_\beta(D|M)} \quad (\text{A.16})$$

with the parameter $\beta \in [0, 1]$. Because $\int p_\beta(\theta|D, M)d\theta = 1$, the evidence is

$$\begin{aligned} p_\beta(D|M) &= \int [p(D|\theta, M)]^\beta p(\theta|M)d\theta \\ &= \int q_\beta(\theta|D, M)d\theta. \end{aligned} \quad (\text{A.17})$$

Taking the derivative $\partial \ln p_\beta(D|M)/\partial\beta = [1/p_\beta(D|M)]\partial p_\beta(D|M)/\partial\beta$ yields

$$\begin{aligned} \frac{\partial \ln p_\beta(D|M)}{\partial\beta} &= \frac{\int \ln p(D|\theta, M)q_\beta(\theta|D, M)d\theta}{\int q_\beta(\theta|D, M)d\theta} \\ &= \int \ln p(D|\theta, M)p_\beta(\theta|D, M)d\theta \\ &= \langle \ln p(D|\theta, M) \rangle_\beta \end{aligned} \quad (\text{A.18})$$

where the mean is intended over the set of parameters θ and with respect to the posterior probability for the model parameters $p_\beta(\theta|D, M)$. The integral $\int_0^1 [\partial \ln p_\beta(D|M)/\partial\beta]d\beta =$

$\ln p_1(D|M) - \ln p_0(D|M) = \ln p(D|M)$ (because $\int p(\theta|M)d\theta = 1$) yields the logarithm of the Bayesian evidence entering the Bayes factor in equation (A.12)

$$\ln p(D|M) = \int_0^1 \langle \ln p(D|\theta, M) \rangle_\beta d\beta. \quad (\text{A.19})$$

A.3 Numerical details

For our Bayesian analysis we use the code APEMoST developed by Johannes Buchner and Michael Gruberbauer [86]. The first version of the code was applied to the analysis of stellar pulsations [87].

We use 2×10^6 MCMC iterations to guarantee a fairly complete sampling of the parameter space and twenty chains or values of $\beta \in [0, 1]$. The boundaries of the parameter space were set to $[-1000, 1000]$ for all the a and b parameters, $[0.01, 1000]$ for the σ_{int} parameters, $[0.01, 1.0]$ for Ω_0 , $[-1, -0.001]$ for q_0 , $[1, 3]$ for a_V , $[3, 30] \times 10^{-5}$ for δ_0 , and $[10^{-5}, 10]$ for $a(t_0)$. The initial seed of the random number generator was set with the `bash` command `GSL_RANDOM_SEED=$RANDOM`.

References

- [1] A. G. Riess, A. V. Filippenko, P. Challis, A. Clocchiatti, A. Diercks, P. M. Garnavich, R. L. Gilliland, C. J. Hogan, S. Jha, R. P. Kirshner, B. Leibundgut, M. M. Phillips, D. Reiss, B. P. Schmidt, R. A. Schommer, R. C. Smith, J. Spyromilio, C. Stubbs, N. B. Suntzeff, and J. Tonry, *Observational Evidence from Supernovae for an Accelerating Universe and a Cosmological Constant*, *Astron. J.* **116** (Sept., 1998) 1009–1038, [[astro-ph/](#)].
- [2] S. Perlmutter, G. Aldering, G. Goldhaber, R. A. Knop, P. Nugent, P. G. Castro, S. Deustua, S. Fabbro, A. Goobar, D. E. Groom, I. M. Hook, A. G. Kim, M. Y. Kim, J. C. Lee, N. J. Nunes, R. Pain, C. R. Pennypacker, R. Quimby, C. Lidman, R. S. Ellis, M. Irwin, R. G. McMahon, P. Ruiz-Lapuente, N. Walton, B. Schaefer, B. J. Boyle, A. V. Filippenko, T. Matheson, A. S. Fruchter, N. Panagia, H. J. M. Newberg, W. J. Couch, and The Supernova Cosmology Project, *Measurements of Omega and Lambda from 42 High-Redshift Supernovae*, *Astroph. J.* **517** (June, 1999) 565–586, [[astro-ph/](#)].
- [3] E. Bianchi and C. Rovelli, *Cosmology forum: Is dark energy really a mystery? "No it isn't"*, *Nature* **466** (July, 2010) 321–+.
- [4] R. Kolb, *Cosmology forum: Is dark energy really a mystery? "Yes it is"*, *Nature* **466** (July, 2010) 321–+.
- [5] E. Bianchi and C. Rovelli, *Why all these prejudices against a constant?*, *ArXiv e-prints* (Feb., 2010) [[arXiv:1002.3966](#)].
- [6] L. Amendola and S. Tsujikawa, *Dark Energy: Theory and Observations*. 2010.
- [7] S. Nojiri and S. D. Odintsov, *Unified cosmic history in modified gravity: from F(R) theory to Lorentz non-invariant models*, *ArXiv e-prints* (Nov., 2010) [[arXiv:1011.0544](#)].
- [8] S. Capozziello and V. Faraoni, *Beyond Einstein Gravity: A Survey of Gravitational Theories for Cosmology and Astrophysics*. 2010.
- [9] J. Dunkley, E. Komatsu, M. R.olta, D. N. Spergel, D. Larson, G. Hinshaw, L. Page, C. L. Bennett, B. Gold, N. Jarosik, J. L. Weiland, M. Halpern, R. S. Hill, A. Kogut, M. Limon, S. S. Meyer, G. S. Tucker, E. Wollack, and E. L. Wright, *Five-Year Wilkinson Microwave Anisotropy Probe Observations: Likelihoods and Parameters from the WMAP Data*, *Astroph. J. Suppl.* **180** (Feb., 2009) 306–329, [[arXiv:0803.0586](#)].

- [10] F. Hoyle and A. Sandage, *The Second-Order Term in the Redshift-Magnitude Relation*, *Publ. Astron. Soc. Pac.* **68** (Aug., 1956) 301–+.
- [11] P. D. Mannheim, *Conformal cosmology with no cosmological constant*, *General Relativity and Gravitation* **22** (Mar., 1990) 289–298.
- [12] P. D. Mannheim, *Cosmic Acceleration as the Solution to the Cosmological Constant Problem*, *Astroph. J.* **561** (Nov., 2001) 1–12, [[astro-ph/](#)].
- [13] P. D. Mannheim, *How Recent is Cosmic Acceleration?*, *International Journal of Modern Physics D* **12** (2003) 893–904, [[astro-ph/](#)].
- [14] E. Costa, M. Feroci, L. Piro, M. N. Cinti, F. Frontera, G. Zavattini, L. Nicastro, E. Palazzi, D. dal Fiume, M. Orlandini, J. in 't Zand, J. Heise, R. Jager, A. Parmar, A. Owens, S. Molendi, G. Cusumano, M. C. Maccarone, S. Giarrusso, L. A. Antonelli, F. Fiore, P. Giommi, J. M. Muller, L. Salotti, G. Gennaro, M. Stornelli, G. Crisigiovanni, R. Ricci, A. Coletta, R. C. Butler, D. A. Frail, and S. R. Kulkarni, *GRB 970228*, *IAU Circ.* **6576** (Mar., 1997) 1–+.
- [15] E. Cohen and T. Piran, *The Implications of Direct Redshift Measurement of Gamma-Ray Bursts*, *Astroph. J. Lett.* **488** (Oct., 1997) L7+, [[astro-ph/](#)].
- [16] J.-L. Atteia, *Gamma-ray bursts: towards a standard candle luminosity*, *Astron. & Astroph.* **328** (Dec., 1997) L21–L24, [[astro-ph/](#)].
- [17] B. Stern, J. Poutanen, and R. Svensson, *A Complexity-Brightness Correlation in Gamma-Ray Bursts*, *Astroph. J.* **510** (Jan., 1999) 312–324, [[astro-ph/](#)].
- [18] J. P. Norris, G. F. Marani, and J. T. Bonnell, *Connection between Energy-dependent Lags and Peak Luminosity in Gamma-Ray Bursts*, *Astroph. J.* **534** (May, 2000) 248–257, [[astro-ph/](#)].
- [19] D. E. Reichart, D. Q. Lamb, E. E. Fenimore, E. Ramirez-Ruiz, T. L. Cline, and K. Hurley, *A Possible Cepheid-like Luminosity Estimator for the Long Gamma-Ray Bursts*, *Astroph. J.* **552** (May, 2001) 57–71, [[astro-ph/](#)].
- [20] B. E. Schaefer, *Gamma-Ray Burst Hubble Diagram to $z=4.5$* , *Astroph. J. Lett.* **583** (Feb., 2003) L67–L70, [[astro-ph/](#)].
- [21] B. E. Schaefer, *The Hubble Diagram to Redshift > 6 from 69 Gamma-Ray Bursts*, *Astroph. J.* **660** (May, 2007) 16–46, [[astro-ph/](#)].
- [22] R. Salvaterra, M. Della Valle, S. Campana, G. Chincarini, S. Covino, P. D’Avanzo, A. Fernández-Soto, C. Guidorzi, F. Mannucci, R. Margutti, C. C. Thöne, L. A. Antonelli, S. D. Barthelmy, M. de Pasquale, V. D’Elia, F. Fiore, D. Fugazza, L. K. Hunt, E. Maiorano, S. Marinoni, F. E. Marshall, E. Molinari, J. Nousek, E. Pian, J. L. Racusin, L. Stella, L. Amati, G. Andreuzzi, G. Cusumano, E. E. Fenimore, P. Ferrero, P. Giommi, D. Guetta, S. T. Holland, K. Hurley, G. L. Israel, J. Mao, C. B. Markwardt, N. Masetti, C. Pagani, E. Palazzi, D. M. Palmer, S. Piranomonte, G. Tagliaferri, and V. Testa, *GRB090423 at a redshift of $z\sim 8.1$* , *Nature* **461** (Oct., 2009) 1258–1260, [[arXiv:0906.1578](#)].
- [23] N. R. Tanvir, D. B. Fox, A. J. Levan, E. Berger, K. Wiersema, J. P. U. Fynbo, A. Cucchiara, T. Krühler, N. Gehrels, J. S. Bloom, J. Greiner, P. A. Evans, E. Rol, F. Olivares, J. Hjorth, P. Jakobsson, J. Farihi, R. Willingale, R. L. C. Starling, S. B. Cenko, D. Perley, J. R. Maund, J. Duke, R. A. M. J. Wijers, A. J. Adamson, A. Allan, M. N. Bremer, D. N. Burrows, A. J. Castro-Tirado, B. Cavanagh, A. de Ugarte Postigo, M. A. Dopita, T. A. Fatkhullin, A. S. Fruchter, R. J. Foley, J. Gorosabel, J. Kennea, T. Kerr, S. Klose, H. A. Krimm, V. N. Komarova, S. R. Kulkarni, A. S. Moskvitin, C. G. Mundell, T. Naylor, K. Page, B. E. Penprase, M. Perri, P. Podsiadlowski, K. Roth, R. E. Rutledge, T. Sakamoto, P. Schady, B. P. Schmidt, A. M. Soderberg, J. Sollerman, A. W. Stephens, G. Stratta, T. N. Ukwatta, D. Watson, E. Westra, T. Wold, and C. Wolf, *A γ -ray burst at a redshift of $z\sim 8.2$* , *Nature* **461** (Oct., 2009) 1254–1257, [[arXiv:0906.1577](#)].

- [24] J. E. Grindlay, *GRB Probes of the Early Universe with EXIST*, in *American Institute of Physics Conference Series* (N. Kawai & S. Nagataki, ed.), vol. 1279 of *American Institute of Physics Conference Series*, pp. 212–219, Oct., 2010. [arXiv:1008.3280](#).
- [25] S. Campana, R. Salvaterra, G. Tagliaferri, C. Kouveliotou, and J. Grindlay, *Probing the very high redshift Universe with gamma-ray bursts: prospects for observations with future X-ray instruments*, *Month. Not. Roy. Astr. Soc.* **410** (Jan., 2011) 1611–1616, [[arXiv:1008.3054](#)].
- [26] G. Ghirlanda, G. Ghisellini, and C. Firmani, *Gamma-ray bursts as standard candles to constrain the cosmological parameters*, *New Journal of Physics* **8** (July, 2006) 123–+, [[astro-ph](#)].
- [27] A. S. Friedman and J. S. Bloom, *Toward a More Standardized Candle Using Gamma-Ray Burst Energetics and Spectra*, *Astroph. J.* **627** (July, 2005) 1–25, [[astro-ph](#)].
- [28] C. Firmani, G. Ghisellini, G. Ghirlanda, and V. Avila-Reese, *A new method optimized to use gamma-ray bursts as cosmic rulers*, *Month. Not. Roy. Astr. Soc.* **360** (June, 2005) L1–L5, [[astro-ph](#)].
- [29] E. Liang and B. Zhang, *Model-independent Multivariable Gamma-Ray Burst Luminosity Indicator and Its Possible Cosmological Implications*, *Astroph. J.* **633** (Nov., 2005) 611–623, [[astro-ph](#)].
- [30] E. Liang and B. Zhang, *Calibration of gamma-ray burst luminosity indicators*, *Month. Not. Roy. Astr. Soc.* **369** (June, 2006) L37–L41, [[astro-ph](#)].
- [31] N. Liang, W. K. Xiao, Y. Liu, and S. N. Zhang, *A Cosmology-Independent Calibration of Gamma-Ray Burst Luminosity Relations and the Hubble Diagram*, *Astroph. J.* **685** (Sept., 2008) 354–360, [[arXiv:0802.4262](#)].
- [32] S. Basilakos and L. Perivolaropoulos, *Testing gamma-ray bursts as standard candles*, *Month. Not. Roy. Astr. Soc.* **391** (Nov., 2008) 411–419, [[arXiv:0805.0875](#)].
- [33] V. F. Cardone, S. Capozziello, and M. G. Dainotti, *An updated gamma-ray bursts Hubble diagram*, *Month. Not. Roy. Astr. Soc.* **400** (Dec., 2009) 775–790, [[arXiv:0901.3194](#)].
- [34] M. Demianski, E. Piedipalumbo, and C. Rubano, *The gamma-ray bursts Hubble diagram in quintessential cosmological models*, *Month. Not. Roy. Astr. Soc.* **411** (Feb., 2011) 1213–1222, [[arXiv:1010.0855](#)].
- [35] G. U. Varieschi, *A kinematical approach to conformal cosmology*, *General Relativity and Gravitation* **42** (Apr., 2010) 929–974, [[arXiv:0809.4729](#)].
- [36] H. Weyl, *Reine Infinitesimalgeometrie*, *Math. Z.* **2** (1918) 384.
- [37] H. Weyl, *Eine neue Erweiterung der Relativitätstheorie*, *Ann. Phys. Lpz.* **364** (1919) 101.
- [38] H. Weyl, *Elektrizität und Gravitation*, *Phys. Z.* **21** (1920) 649.
- [39] P. D. Mannheim, *Linear Potentials and Galactic Rotation Curves*, *Astroph. J.* **419** (Dec., 1993) 150–+, [[hep-ph/92](#)].
- [40] P. D. Mannheim, *Are Galactic Rotation Curves Really Flat?*, *Astroph. J.* **479** (Apr., 1997) 659, [[astro-ph](#)].
- [41] P. D. Mannheim and J. G. O’Brien, *Fitting galactic rotation curves with conformal gravity and a global quadratic potential*, *ArXiv e-prints* (Nov., 2010) [[arXiv:1011.3495](#)].
- [42] P. D. Mannheim, *Conformal Gravity Challenges String Theory*, in *2nd Crisis in Cosmology Conference* (F. Potter, ed.), vol. 413 of *Astronomical Society of the Pacific Conference Series*, pp. 279–+, Dec., 2009.
- [43] P. D. Mannheim, *Comprehensive solution to the cosmological constant, zero-point energy, and quantum gravity problems*, *General Relativity and Gravitation* **43** (Mar., 2011) 703–750,

- [arXiv:0909.0212].
- [44] C. M. Bender and P. D. Mannheim, *No-Ghost Theorem for the Fourth-Order Derivative Pais-Uhlenbeck Oscillator Model*, *Physical Review Letters* **100** (Mar., 2008) 110402–+, [arXiv:0706.0207].
- [45] L. Knox and A. Kosowsky, *Primordial nucleosynthesis in conformal Weyl gravity*, tech. rep., Oct., 1993.
- [46] D. Elizondo and G. Yepes, *Can conformal Weyl gravity be considered a viable cosmological theory?*, *Astroph. J.* **428** (June, 1994) 17–20, [astro-ph/].
- [47] K. Jedamzik, *Cosmological deuterium production in non-standard scenarios*, *Planetary and Space Science* **50** (Oct., 2002) 1239–1244, [astro-ph/].
- [48] G. U. Varieschi, *Conformal Cosmology and the Pioneer Anomaly*, *ArXiv e-prints* (Oct., 2010) [arXiv:1010.3262].
- [49] P. D. Mannheim, *Conformal gravity and the flatness problem*, *Astroph. J.* **391** (June, 1992) 429–432.
- [50] P. D. Mannheim, *Alternatives to dark matter and dark energy*, *Progress in Particle and Nuclear Physics* **56** (Apr., 2006) 340–445, [astro-ph/].
- [51] S. Weinberg, *Gravitation and Cosmology: Principles and Applications of the General Theory of Relativity*. July, 1972.
- [52] M. D. Lehnert, N. P. H. Nesvadba, J.-G. Cuby, A. M. Swinbank, S. Morris, B. Clément, C. J. Evans, M. N. Bremer, and S. Basa, *Spectroscopic confirmation of a galaxy at redshift $z = 8.6$* , *Nature* **467** (Oct., 2010) 940–942, [arXiv:1010.4312].
- [53] G. U. Varieschi, *Kinematical Conformal Cosmology: fundamental parameters from astrophysical observations*, *ArXiv e-prints* (Dec., 2008) [arXiv:0812.2472].
- [54] J. D. Anderson, P. A. Laing, E. L. Lau, A. S. Liu, M. M. Nieto, and S. G. Turyshev, *Study of the anomalous acceleration of Pioneer 10 and 11*, *Phys. Rev. D* **65** (Apr., 2002) 082004–+, [gr-qc/010].
- [55] F. Francisco, O. Bertolami, P. J. S. Gil, and J. Páramos, *Modelling the reflective thermal contribution to the acceleration of the Pioneer spacecraft*, *ArXiv e-prints* (Mar., 2011) [arXiv:1103.5222].
- [56] S. G. Turyshev, V. T. Toth, J. Ellis, and C. B. Markwardt, *Support for Temporally Varying Behavior of the Pioneer Anomaly from the Extended Pioneer 10 and 11 Doppler Data Sets*, *Physical Review Letters* **107** (Aug., 2011) 081103–+, [arXiv:1107.2886].
- [57] G. D’Agostini, *Fits, and especially linear fits, with errors on both axes, extra variance of the data points and other complications*, *ArXiv Physics e-prints* (Nov., 2005) [physics/0].
- [58] S. Andreon and M. A. Hurn, *The scaling relation between richness and mass of galaxy clusters: a Bayesian approach*, *Month. Not. Roy. Astr. Soc.* **404** (June, 2010) 1922–1937, [arXiv:1001.4639].
- [59] U.-L. Pen, *Analytical Fit to the Luminosity Distance for Flat Cosmologies with a Cosmological Constant*, *Astroph. J. Suppl.* **120** (Jan., 1999) 49–50, [astro-ph/].
- [60] W. L. Freedman and B. F. Madore, *The Hubble Constant*, *Ann. Rev. Astron. & Astroph.* **48** (Sept., 2010) 673–710, [arXiv:1004.1856].
- [61] L. Xiao and B. E. Schaefer, *Estimating Redshifts for Long Gamma-Ray Bursts*, *Astroph. J.* **707** (Dec., 2009) 387–403, [arXiv:0910.4945].
- [62] M. M. Phillips, *The absolute magnitudes of Type IA supernovae*, *Astroph. J. Lett.* **413** (Aug., 1993) L105–L108.

- [63] M. Kowalski, D. Rubin, G. Aldering, R. J. Agostinho, A. Amadon, R. Amanullah, C. Balland, K. Barbary, G. Blanc, P. J. Challis, A. Conley, N. V. Connolly, R. Covarrubias, K. S. Dawson, S. E. Deustua, R. Ellis, S. Fabbro, V. Fadeyev, X. Fan, B. Farris, G. Folatelli, B. L. Frye, G. Garavini, E. L. Gates, L. Germany, G. Goldhaber, B. Goldman, A. Goobar, D. E. Groom, J. Haissinski, D. Hardin, I. Hook, S. Kent, A. G. Kim, R. A. Knop, C. Lidman, E. V. Linder, J. Mendez, J. Meyers, G. J. Miller, M. Moniez, A. M. Mourão, H. Newberg, S. Nobili, P. E. Nugent, R. Pain, O. Perdureau, S. Perlmutter, M. M. Phillips, V. Prasad, R. Quimby, N. Regnault, J. Rich, E. P. Rubenstein, P. Ruiz-Lapuente, F. D. Santos, B. E. Schaefer, R. A. Schommer, R. C. Smith, A. M. Soderberg, A. L. Spadafora, L.-G. Strolger, M. Strovink, N. B. Suntzeff, N. Suzuki, R. C. Thomas, N. A. Walton, L. Wang, W. M. Wood-Vasey, and J. L. Yun, *Improved Cosmological Constraints from New, Old, and Combined Supernova Data Sets*, *Astroph. J.* **686** (Oct., 2008) 749–778, [[arXiv:0804.4142](#)].
- [64] R. Tripp, *A two-parameter luminosity correction for Type IA supernovae*, *Astron. & Astroph.* **331** (Mar., 1998) 815–820.
- [65] M. Hicken, W. M. Wood-Vasey, S. Blondin, P. Challis, S. Jha, P. L. Kelly, A. Rest, and R. P. Kirshner, *Improved Dark Energy Constraints from ~ 100 New CfA Supernova Type Ia Light Curves*, *Astroph. J.* **700** (Aug., 2009) 1097–1140, [[arXiv:0901.4804](#)].
- [66] A. G. Riess, L. Macri, S. Casertano, M. Sosey, H. Lampeitl, H. C. Ferguson, A. V. Filippenko, S. W. Jha, W. Li, R. Chornock, and D. Sarkar, *A Redetermination of the Hubble Constant with the Hubble Space Telescope from a Differential Distance Ladder*, *Astroph. J.* **699** (July, 2009) 539–563, [[arXiv:0905.0695](#)].
- [67] M. C. March, R. Trotta, P. Berkes, G. D. Starkman, and P. M. Vaudrevange, *Improved constraints on cosmological parameters from SNIa data*, *ArXiv e-prints* (Feb., 2011) [[arXiv:1102.3237](#)].
- [68] L. Amendola, M. Gasperini, and F. Piazza, *Supernova Legacy Survey data are consistent with acceleration at $z \sim 3$* , *Phys. Rev. D* **74** (Dec., 2006) 127302–+, [[astro-ph/](#)].
- [69] H. Jeffreys, *Theory of Probability*. 1961.
- [70] R. Trotta, *Applications of Bayesian model selection to cosmological parameters*, *Month. Not. Roy. Astr. Soc.* **378** (June, 2007) 72–82, [[astro-ph/](#)].
- [71] M. Aitkin, *Posterior Bayes factor*, *Journal of the Royal Statistical Society, Series B (Methodological)* **53** (1991) 111–142.
- [72] R. E. Kass and A. E. Raftery, *Bayes factors*, *Journal of the American Statistical Association* **90** (1995) 773–795.
- [73] D. L. Weakliem, *A critique of the Bayesian information criterion for model selection*, *Sociological Methods and Research* **27** (Feb., 1999) 359–397.
- [74] J. O. Berger and L. R. Pericchi, *Objective Bayesian methods for model selection: introduction and comparison*, *Lecture Notes-Monograph Series - Model Selection* **38** (2001) 135–207.
- [75] V. E. Johnson, *Bayes factors based on test statistics*, *Journal of the Royal Statistical Society, Series B (Statistical Methodology)* **67** (2005) 689–701.
- [76] C. C. Liu and M. Aitkin, *Bayes factors: prior sensitivity and model generalizability*, *Journal of Mathematical Psychology* **52** (2008) 362–375.
- [77] H. Li, J.-Q. Xia, J. Liu, G.-B. Zhao, Z.-H. Fan, and X. Zhang, *Overcoming the Circular Problem for Gamma-Ray Bursts in Cosmological Global-Fitting Analysis*, *Astroph. J.* **680** (June, 2008) 92–99, [[arXiv:0711.1792](#)].
- [78] L.-X. Li, *Are Gamma-Ray Bursts a Standard Energy Reservoir?*, *Acta Astronomica* **58** (June, 2008) 103–112, [[arXiv:0806.2770](#)].

- [79] S. McBreen, T. Krühler, A. Rau, J. Greiner, D. A. Kann, S. Savaglio, P. Afonso, C. Clemens, R. Filgas, S. Klose, A. Küpcü Yoldaş, F. Olivares E., A. Rossi, G. P. Szokoly, A. Updike, and A. Yoldaş, *Optical and near-infrared follow-up observations of four Fermi/LAT GRBs: redshifts, afterglows, energetics, and host galaxies*, *Astron. & Astroph.* **516** (June, 2010) A71, [[arXiv:1003.3885](https://arxiv.org/abs/1003.3885)].
- [80] A. Shahmoradi and R. J. Nemiroff, *The possible impact of gamma-ray burst detector thresholds on cosmological standard candles*, *Month. Not. Roy. Astr. Soc.* **411** (Mar., 2011) 1843–1856.
- [81] K. Horne, *X-ray gas in the galaxy cluster Abell 2029: conformal gravity versus dark matter*, *Month. Not. Roy. Astr. Soc.* **369** (July, 2006) 1667–1676.
- [82] A. Diaferio and L. Ostorero, *X-ray clusters of galaxies in conformal gravity*, *Month. Not. Roy. Astr. Soc.* **393** (Feb., 2009) 215–223, [[arXiv:0808.3707](https://arxiv.org/abs/0808.3707)].
- [83] P. D. Mannheim, *Making the Case for Conformal Gravity*, *ArXiv e-prints* (Jan., 2011) [[arXiv:1101.2186](https://arxiv.org/abs/1101.2186)].
- [84] R. Trotta, *Bayes in the sky: Bayesian inference and model selection in cosmology*, *Contemporary Physics* **49** (Mar., 2008) 71–104, [[arXiv:0803.4089](https://arxiv.org/abs/0803.4089)].
- [85] M. P. Hobson and C. McLachlan, *A Bayesian approach to discrete object detection in astronomical data sets*, *Month. Not. Roy. Astr. Soc.* **338** (Jan., 2003) 765–784, [[astro-ph/0301001](https://arxiv.org/abs/astro-ph/0301001)].
- [86] J. Buchner and M. Gruberbauer, “Apemost (automated parameter estimation and model selection toolkit).” <http://apemost.sourceforge.net/>, 02, 2011. commit from 2011-02-10.
- [87] M. Gruberbauer, T. Kallinger, W. W. Weiss, and D. B. Guenther, *On the detection of Lorentzian profiles in a power spectrum: a Bayesian approach using ignorance priors*, *Astron. & Astroph.* **506** (Nov., 2009) 1043–1053, [[arXiv:0811.3345](https://arxiv.org/abs/0811.3345)].